This is to certify that the

thesis entitled

AN EVALUATION OF THE PARAMETERS
INVOLVED IN DEVELOPING A RADIOTRACER
BASED WEAR DIAGNOSTICS SYSTEM

presented by

Dick A. Barkman

has been accepted towards fulfillment
of the requirements for

MS degree in Mechanical Engineering

Harold J. Schock
Major professor

Date 7/4/92

AN EVALUATION OF THE PARAMETERS INVOLVED IN DEVELOPING A RADIOTRACER BASED WEAR DIAGNOSTICS SYSTEM

By

Dick A Barkman

A THESIS

Submitted to
Michigan State University
in partial fulfillment of the requirements
for the degree of

Master of Science

Department of Mechanical Engineering

1992

ABSTRACT

AN EVALUATION OF THE PARAMETERS INVOLVED IN DEVELOPING A RADIOTRACER BASED WEAR DIAGNOSTICS SYSTEM

By

Dick A Barkman

Wear is an important parameter in the design and operation of mechanical systems. Wear can cause catastrophic failure of mechanical components, costing manufacturers and users alike due to lost production or service time. Non-intrusive radiotracer systems provide a means of getting wear data in a short time while the target equipment is still in operation. The purpose of this study was to investigate the parameters involved in developing and operating a system that monitors wear on line. To this end, a system was designed and built to measure the piston ring wear of an internal combustion engine. A one cylinder engine was modified so that its oil supply could be pumped to an external reservoir and back in a closed circuit. The external reservoir enables one to measure radioactive material in the oil. Then, a radioactive piston ring was installed in the engine. As the engine ran, radioactive particles were worn off of the piston ring and mixed into the oil. Finally, a gamma ray detection system was set up to measure the amounts of radiation in the oil and piston ring. Wear rates were calculated from these measurements.

Approved by:

Major Professor

ACKNOWLEDGEMENTS

To my parents, for the support, financial and otherwise, which made it possible for me to reach my goals.

To Dr. Schock, for finding financial support for me where there was none, and for making this project possible.

To Dr. Somerton and Dr. Radcliffe, for being on my commitee on such short notice.

To Dr. Ronningen, for the careful instruction on radiation, gamma ray detectors, and numerous other subjects which made this project possible.

To Tom Stuecken, for providing the practical side of my education, and for the numerous favors without which I may never have finished.

Special thanks to Bruce Henderson, Chris Heintzman, and the rest of the M.S.U. Karate Club without whom this would have been done a lot sooner.

TABLE OF CONTENTS

LIST OF TABLES

LIST OF FIGURES

Page

CHAPTER 1

INTRODUCTION

1.1 Problem Statement

Wear is an important parameter in the design and operation of mechanical systems. Wear can cause catastrophic failure of mechanical components, costing manufacturers and civilians alike in lost production or service time. It is often cheaper to invest in wear prevention methods than it is to repair damaged equipment. Wear prevention requires knowing how much wear is critical, what conditions cause the most wear, and where it happens. One way to acquire this information is to periodically disassemble the equipment and measure the parts of concern. This method has serious drawbacks. It causes expensive downtime of equipment, reassembly of equipment changes the subsequent wear pattern, and the method is limited to relatively large amounts of wear. For industries that cannot afford the downtime of equipment and/or need more precise measurements of wear, a better alternative is the non-intrusive radiotracer method. This method provides a means of getting wear data in a short time, while the target equipment is still in operation. This method, however, is not currently commercially available in the United States. The purpose of this study was to determine what is involved in designing, building, and operating a system that monitors wear on-line. In particular, this system was designed to measure piston ring wear in an internal combustion engine by rendering a section of the surface of a piston ring radioactive, installing it in a test engine, and monitoring the radiation over a period of test runs. The amount of radiation left on the ring is directly related to the amount of wear that has taken place.

1.2 Literature Survey

Much research has been done on wear prediction and measurement. The radionuclide technique is getting an increasng amount of attention from industry and university researchers alike. The following papers illustrate the wide range of application of the radionuclide technique.

Evans [1] compared the surface layer activation (SLA) method with a nuetron activation method for wear studies. It was found that SLA had several advantages over the nuetron method: A much lower activity of the sample was possible with SLA, irradiation of only the area of interest was possible, and SLA provides a choice of radionuclides to use.

Kinsella et al [2] used the radiotracer method to study the material removal process in the sliting of cast iron. The method was found to be suitable for tracing wear debris in adhesive and abrasive processes. Slitting was studied at low and high loads. At low loads all the slit cast iron was transferred to the rim by adhesion, oxidized, and escaped from the system as debris. At high loads the iron transferred to the rim became hard and abrasive. In this case half the slit volume of material became debris directly by abrasion rather than the adhesive transfer to, and decay from , the rim, as evident in the low load case.

Fritz et al [3] performed in situ piston ring wear measurements in a medium speed diesel engine. The research engine was a single cylinder model run at conditions simulating the operation of line haul locomotives. Data was taken at various speeds and loads by both the radiotracer and radiomarker methods. The high correlation in the data from both methods was taken to indicate that monitoring wear in situ is sufficient and that stopping the engine for direct measurements is unnecessary.

Schneider and Blossfeld [4] did a comprehensive study of the effect of speed and power output on piston ring wear in a Detriot Deisel "series 60" engine. The radiotracer and marker method were used with radioactive ^{54}Mn being the nuclide used. Rings were activated circumferrentially and in discrete bands while wear rates were measured at 21 different test conditions. It was determined that at constant powerwear rates increase with decreasing speed, and at all speeds the wear rates increased with increased power output and BMEP.

CHAPTER 2

CONCEPTS IN RADIATION DETECTION

2.1 Outline of Wear Measurement Methods

For wear analysis, two methods are currently used to render a piston ring radioactive. The first method, called surface layer activation (SLA), is only useful on certian materials with atomic number greater than 24. In SLA, a piston ring is bombarded with energetic particles, causing nuclear reactions. These reactions change the iron to cobalt 56, a radioactive element. A second method, which involves direct ion implantation, has the advantage that it works on any material. In this method, radioactive particles are implanted into the ring.

Once the radioactive ring is installed in the test engine, there are two ways to detect piston ring wear: the marker method and the tracer method. In the marker method (Figure 2.1 A), the level of the ring radiation is measured directly through the engine block between intervals of engine operation. The difference in the levels of radiation measured before and after a run are directly related to the amount of wear on the piston ring. In the tracer method, the radiation in the oil is related to the amount of material worn off the ring. The tracer method (Figure 2.1 B) has the advantages that it can be used while the engine is running and the detector can be located some distance away from the engine. If the detector is close to the engine, the vibration will cause system noise which decreases the detector resolution. The marker method allows for faster measurements, but this method requires that the engine be stopped and the piston be at a fixed position relative to the detector. For comparison, both types of measurement were used in this study. The gamma radiation emitted by the ring can penetrate most materials with very little attenuation compared to charged particle radiation (such as alpha and beta particles) and is easily identified from background radiation.

Once the radiation has been measured, the wear can be determined by using the depth calibration curve shown in Figure 2.2. The relative intensity is the ratio of the radiation measured after a period of engine operation to the radiation measured before. This depth calibration is produced by removing thin layers of surface material from an activated control piston ring and measuring the difference in radiation produced. Surface material is removed by masking around the activated region and sand blasting. The activity remaining is then measured, while the roundness profilometry is used to determine the surface thickness removed. Roundness profilometry measures the height of the step between masked and unmasked regions.

2.2 Radiation Terms and Definitions

Familiarity with the atom is necessary to understand how gamma radiation is produced. The atom has a nucleus consisting of protons that are positively charged and neutrons that have no charge. Electrons, which are negatively charged, orbit about this nucleus. Each individual combination of protons and neutrons is called an element, or nuclide. Figure 2.3 represents a basic atom.

Nuclides that differ only in the number of neutrons are called isotopes of one another. The number of protons in the atom gives each nuclide its chemical identitity. Most nuclides are unstable (radioactive). Radioactivity is defined as the spontaneous disintegration of unstable nuclei with the resulting emission of nuclear energy that results in the formation of new elements. There are many modes of disintegration, or decay, but only one shall be dicussed here: gamma ray emission.

Gamma ray emission is the production of electromagnetic radiation by a nucleus that is reconFigureuring to reach its lowest energy state. Radioactive nuclides give off gamma rays only at a specific pattern of energies and intensities characteristic of that nuclide. Cobalt 56, for instance, is the only nuclide to give off gamma rays at 846 keV, 1038 keV, 1237 keV, and 1771 keV, a pattern which no other nuclide shares. The intensity of the gamma rays given off at these energies is also unique to cobalt 56.

The activity of a radioactive sample is the instantaneous number of atoms decaying per unit time. Activity is measured in Becquerels (Bq), where one Bq is one disintegration per second. The curie is a unit more commonly used. One curie is equivalent to 3.7x10^10 disintegrations per second (d.p.s.). Only a fraction of the decays occurring give off gamma radiation because a nucleus may decay in many different ways. The branching ratio is the probabiltity, expressed in percents, that a nucleus, or the excited state of a nucleus, will decay in a particular manner. This branching ratio is given in gamma rays per 100 decays. Figure 2.4 shows the decay paths for 7Be. There is an 89.7 percent chance that it will decay directly to the ground state of lithium 7, and a 10.3% chance tha it will decay to the excited state of 7Li. The excited state of 7Li will decay to the ground state by releasing a gamma ray. The branching ratio is then the number of gamma rays given off per 100 decays, which is 10.3.

Radioactive nuclides disintegrate spontaneously at a rate that is dependent on the number of original atoms present and upon its decay constant lambda, λ . This constant λ is defined as the instantaneous fraction of atoms decaying per unit time. Each nuclide has its own characteristic decay constant. The relation between the number of atoms left at a given time and the original number of atoms is given by the decay equation:

$$N_t = N_o * e^{-\lambda t} \tag{2.1}$$

N_t is the number of atoms present at some time t and N_o is the original number of atoms present. The decay constant, λ, is related to the nuclides halflife, $T_{1/2}$, by the equation:

$$\lambda = \ln 2 / T_{1/2}. \tag{2.2}$$

The halflife is the time it takes for the number of atoms to decay to one half of the original amount. The instantaneous number of atoms, N, remaining at a given time is given by:

$$N = A / \lambda, \tag{2.3}$$

where A is the activity. The decay equation is important for wear stufies because the differnce in the level of radiation being measured is partly due to wear and partly due to natural decay. The amount of material that has decayed must be accounted for in order to get an accurate assesment of the wear.

Activity is measured by using a gamma ray detector. A detector counts the number of photons given off by a radioactive source at specific energy levels. The activity is calculated by dividing the total number of photons given off at a specific energy by the time spent counting. Only a fraction of the photons given off at any discrete energy levels are gamma photons, as discussed earlier. Since only gamma photons are being counted, the total number of photons at a specific energy must be calculated by dividing the number of gamma photons counted at that energy by the branching ratio for that energy. A typical gamma ray spectrum for a count of a cobalt source is shown in Figure 2.5.

Four cobalt peaks are shown in the Figure. The activity of the source can be calculated from any one of the peaks by the following equation:

$$\text{Activity} = \frac{\text{peak area}}{(\text{livetime})(\text{branching ratio})(\text{efficiency})} \tag{2.4}$$

The peak area is the total number of photons detected above the background energy level at one energy. The live time is the time spent counting. The efficiency is the efficiency of the detector and is given by:

$$\text{Total Efficiency} = \frac{\text{number of photons emitted by the source}}{\text{number of signals generated by the detector}} \tag{2.5}$$

Ideally the calculated activity would be the same no matter which peak area was used. This is not the case, however, due to uncertianties in the counting. To approximate the true activity the mean of the activities calculated at each peak energy is used:

$$\text{Mean activity} = \frac{\Sigma(\text{activity}_i \,/\, \text{activity error}_i^{\,2})}{\Sigma(1 \,/\, \text{activity error}_i^{\,2})}\text{, and} \tag{2.6}$$

$$\text{Mean activity error} = \frac{1}{[\,\Sigma(\,1 \,/\, \text{activity error}_i^{\,2}\,)]^{1/2}}\,. \tag{2.7}$$

CHAPTER 3

SYSTEM IMPLEMENTATION

3.1 Overall design

Figure 3.1 shows a schematic of the system design. A dynamometer, engine stand, engine, and pump are mounted on a rolling table. The pump and engine are connected to the oil reservoir by flexible hose (not shown). The dynamometer is linked to the engine by a rubber coupling on the crankshaft. The dynamometer has a separate controller mounted on its own mobile stand. The detector is connected to the multi-channel analyzer (MCA) and personal computer by long cables. Every 24 hours, the detector dewar is filled with liquid nitrogen from a 50 liter tank. The details of each system component are given below.

3.2 Individual System Components

3.2.1 Piston Ring

In the present study, SLA was used on the top compression ring by Kernforschungszentrum, a cyclotron in Germany. For this type of study the ring can rotate in its groove, therfore it is necessary to either activate the entire surface of the ring or to activate a portion of the surface and pin the ring so that it cannot rotate. The ring must not rotate when only a section is activated because the activate portion must remain in a fixed orientation relative to the gamma ray detector positioned outside the engine. To avoid the expense of a full activation the ring was pinned in the present study. The ring was activated in a 10 x 1.5 milimeter area 90 degrees from the ring gap as measured looking down on the beveled surface. The ring had an activity of 7.5 microcuries.

3.2.1 Test Engine

The test engine is shown in Figure 3.2. It is a 6.2 kw (11 h.p.)

Briggs & Stratton with an aluminum block and cast iron bore. It is a single cylinder model meant for running pumps and other industrial equipment.

To calculate the total amount of radioactivity in the oil from a measurement of a fraction of the oil, the oil must be homogeneously radioactive. The location of the engine block oil ports, however, tends to minimize mixing of the oil. These ports face each other across the crankcase creating the possibility that return oil could bypass mixing with the more radioactive oil and go right back to the reservoir. To eliminate this problem a steel baffle was placed in the crankcase in front of the oil return port to circulate the oil.

Later in the study the engine compression ratio was raised in the hopes of increasing the wear rate. Since the engine instruction manual did not give the stock compression ratio, it was measured using the water displacement principal to be 7.6. The head was then machined to a new compression ratio of 9.5.

3.2.1.1 The Dynamometer

For this study, the engine speed and load had to be carefully controlled. A 50 h.p. eddy current dynamometer was used for this purpose. It has three basic functions: to drive an engine, for either non-firing tests or starting; to carefully load the engine; and to monitor the engine speed and torque output.

The test engine was a pull-start model. Instead of using a pull-start for the tests, however, the dynamometer was used to crank the engine over until it fired. Once the engine fired, the dynamometer stopped driving it and began absorbing its output, monitoring the load in the process. If a load needs to be placed on the engine, there are two ways the dynamometer can load it: It can put a load that varies as necessary to hold the engine at a constant speed, or it can put a constant load on the engine while the engine speed is free to vary. The dynamometer is shown in Figure 3.3.

The dynamometer shaft is connected to the engine crankshaft through a rubber coupling, shown in Figure 3.4. This coupling protects the dynamometer from being damaged should the engine seize up, or the engine from being damaged by a dynamometer failure. Couplings can be broken by putting a high enough load on the engine to stall it. This load will be high enough to destroy the coupling. The dynamometer operating procedure is in the appendix.

3.2.2 Oil system

To minimize errors in radioactive tracer studies, it is important to minimize the amount of air in the lines and to keep a constant flow of oil. Air bubbles in the line will eventually displace oil in the reservoir during a count of its activity resulting in an erroneous calculation of total activity and thus piston ring wear [7]. An intermittent flow of oil can allow buildup of radioactive particles at different areas in the system resulting in inhomogeneously radioactive oil. As mentioned earlier (Section 3.2.1) homogeneous oil radioactivity is necessary for accurate calculation of activity.

To minimize air bubbbles the system was designed to operate at 70 psi (the optimum pressure for reducing air bubbles [7]), and a gear type pump was used to minimize cavitation. The pump was a 1/3 h.p. adjustable relief valve model with 1/4" ports and a free flow rate of 2.2 gpm of 72 degree water. It was found that cavitation could be reduced by using 1/2" i.d. oil supply lines to the pump, as the pump seemed to draw oil at a greater flow rate than the 1/4" lines would allow. 1/4" lines were originally used because they matched the pump port size.

In order to maintain an oil pressure of 70 psi in the reservoir and lines a relief valve was placed downstream of the reservoir before the return to the crankcase. Another relief valve, which is built into the pump, allows the pump to circulate oil around its own case if the line pressure after the pump gets too high (for example if the lines were pinched shut).

Brass fittings are used to connect the system's elements. Fittings must be chosen that minimize leaks and allow the oil to flow as unrestricted as possible. Fittings can leak under heavy use, so minimizing the number of joints is of prime importance. For example, a street elbow can be used to replace an elbow and bushing to eliminate one joint. To stop leakage the joints must be silver soldered. Regular solder is less effective. For sensitive fittings that cannot be soldered, such as gauges and valves, teflon tape should be wrapped around the threads. Fittings that attach directly to the pump, which has small ports, should be as large as possible to avoid constriction of the flow.

3.2.3 Engine Stand

The engine stand, shown in Figure 3.5, was built to rigidly support the engine so that the engine crankshaft was in line with the dynamometer shaft. It also served as a mount for the pump and relief valve. The stand has low walls around its base to capture any oil that escapes the engine.

3.2.4 Gamma Ray Detector

The gamma ray detector, shown in Figure 3.6, is a high purity germanium coaxial photon detector, manufactured by EG&G Ortec, model number Gem 90220-p-Plus. The detector contains a single crystal of germanium, 75.8 mm in diameter and 92.9 mm in length located in the center of the cylinder 3 mm from the end cap of the detector. This crystal produces electron hole pairs by absorbing gamma ray photons. These electron hole pairs are swept across a 2500 volt electric field inducing a current, that is sent to the preamplifier. Once the preamplifier, which is also under the detector sheath, receives a signal from the crystal; it boosts it and sends it on to the amplifier.

This detector requires low temperatures in order to operate with high resolution. In fact, the crystal and the preamplifier FET (field effect transistor) have to be kept close to liquid nitrogen temperatures in order to reduce thermally induced noise. Thermally induced noise is current generated by the motion of electrons that are excited to the conduction energy level by the ambient temperature. This current is indistinguishable from that produced by incident gamma rays. A high voltage applied to the crystal and the preamplifier FET at higher than liquid nitrogen temperatures could damage them. If the temperature gets too high, a connection is made from the "bias shutdown" output of the preamplifier to the power supply "inhibit", which will shut down the detector. If such a shut down should occur, the detector power supply reading will drop to zero volts. Despite this, the dial will still be set at 2500 volts, so the meter should be checked for power status, not the dial. When such a shutdown occurs the dial should be turned to zero and the "power on" switch turned off. The detector dewar should then be filled with liquid nitrogen in order to cool down for at least 12 hours before the next use.

The cryostat is the device that keeps the crystal at low temperatures. It provides a path for heat transfer from the high vacuum around the crystal to the liquid nitrogen in the dewar. The dewar, which is connected to the detector, contains three liters of liquid nitrogen. Because this nitrogen evaporates very quickly the dewar must be refilled every 24 hours in order to keep the crystal cool.

The system used to fill the dewar consists of an automatic fill controller and a 50 liter tank of LN_2. The auto-fill controller automatically opens, at pre-set times, a solenoid controlled valve between the 50 liter tank and the dewar. The tank was filled at the Michigan State University National Superconducting Cyclotron facilities once a week during everyday operation. When the tank is filled the relief valve will be constantly hissing as it relieves pressure buildup. The tank has a self pressurizing feature that creates large pressures from the nitrogen vapor instantly. Opening the black knob on the top of the tank will activate this system and may form ice on the tank. The self pressurizing function is normally not needed as the relief valve can be used to get a higher pressure, although it takes longer for the pressure to build up.

The auto fill controller, shown in Figure 3.7, is located in the power supply bin with the rest of the electronic equipment. The display on top of the controller shows the amount of time left until the next fill. The green light bulb labeled "filling" below the l.e.d. display lights up when the detector is being filled. The button labelled "manual" opens the solenoid valve no matter where in the countdown process the controller is. The norm/ inhibit switch allows normal operation when set to norm and when set to inhibit prevents the valve from being opened either manually or automatically. The maximum time the controller holds the valve open can be set by dip switches on the side (which can only be seen when the controller is removed from the bin). If this time is exceeded the detector will activate an alarm which sounds until the alarm reset button is pushed. The preset time should not be less than the time it takes for the dewar to fill. When filling is in progress the vent line sends out a stream of vapors. When the dewar becomes full, liquid comes out the vent line (Figure 3.8 A & B). The controller uses a temperature sensor in the dewar vent line to tell when the dewar is full. When the liquid strikes the sensor, the sensor resistance is reduced. When this happens the controller closes the valve. The sensitivity of the controller can be adjusted, but it must be done with care. If it becomes too sensitive the valve will be shut off by just the presence of vapor in the line. If it is adjusted too much the other way the liquid itself will not cause the valve to shut and the liquid will keep venting until the 50 liter tank is empty.

Power can only be applied to the detector when it is cool. This should be at least 12 hours after filling the dewar from a warm state. To do this, it is necessary to turn on the detector power supply, unlock the main power dial, and slowly turn the dial, thus increasing the voltage until a positive 2500 volts is reached. This should be done at a rate of 100 volts per second. Only a low current power supply (micro amp level) should be used. The present study used a Canberra model 3105, 0-5kv power supply that could deliver up to 100 mA of current.

3.2.5 Oil Reservoir

The purpose of the oil reservoir is to contain a fraction of the system oil in such a way as to enable efficient counting of the radiation in the oil. Because the counting time is high when the amount of radiation being measured is low, the reservoir was built to contain a large fraction of the oil to reduce counting times. It was also designed to surround the detector with oil so the geometric efficiency would be high.

Figure 3.9 shows the reservoir, a double coil of copper tubing into which the detector slides. Because of its close proximity to the detector the reservoir had to be designed so that it would not heat the detector. For this purpose two layers of galvanized steel sandwiching a layer of fiberglass insulation were placed on the inside. For additional protection a small blower was used to circulate air between the detector and and the insides of the insulation.

To accurately compare one radiation measurement from the reservoir to the next, the reservoir and detector must be in the same relative position for each measurement. This was ensured by the reservoir-detector stand as shown in Figure 3.10 . The coil slips inside the restraining bars and is bolted in while the detector base slides into the carefully positioned grooves. A metal stop keeps the detector in this reference position for measurement.

3.2.6 Oil Reservoir Platform

A location was needed to keep the coil and detector so that they would not be accidentally damaged. The location also had to have enough room for 260 lbs of lead brick used to shield the detector from the direct path of photons from the engine block. To accomodate the hose used in this system and the lack of space in the engine lab, a rolling table was made to hold the coil, detector, and lead bricks. The oil reservoir platform is shown in Figures 3.11A and B.

The reservoir detector stand bolts down to the base while lead shielding is bolted down next to it, slightly offset to keep the center of mass near the geometric center. The shielding and coil were placed on the lower shelf so that the center of gravity would be low and the risk of the table falling over would be minimized.

3.2.7 Exhaust Stack

Safety regulations dictate that the emission of exhaust take place where it cannot return into a building containing people. Therefore an exhaust stack was built to channel the exhaust to a safe height, 15 feet above the roof of the Engine Research Laboratory. The stack was fabricated out of an aluminum tube. Brackets were made to hold the tube against the side of the bulding, and a short length of tube was welded onto the lower end giving it an L shape for ease of connection to the exhaust flex tube running from the engine. A steel cap was attached to the top to keep rain from entering the tube.

3.2.8 Exhaust Monitoring System

Testing a radioactive piston ring in a running engine creates the possibility that some of the radioactive particles will be swept out the exhaust. If so, this may pose an environmental hazard. One way to deal with this hazard is to pump air into the exhaust to dilute the concentration down to acceptable levels. This is an expensive and unelegant solution because the total amount of hazardous material put into the air remains the same. To fully understand the issue, the amount of radiation in the exhaust was measured during the piston ring break-in period (where the wear is the highest).

This test consisted of placing filters in the exhaust line to trap particulates. To this end, three filter systems were designed, but only one was used. The first two filters were of glass wool, and the third filter was a HEPA filter normally used for gas masks. The glass wool seemed to be the ideal filter but it was discovered that there was no convenient way of determining the efficiency in trapping particulates. The HEPA filter, however, had a well known efficiency of 99%. The disadvantage of this filter was that it was too small and too efficient to be placed directly in the exhaust flow without stalling the engine. The problem was solved by drawing off a portion of the exhaust gas through the HEPA filter with a vacuum pump.

The glass wool used for the first two filters had to completely filter the exhaust. The container shown below was built to hold the glass wool against the pressure of the exhaust gases while not allowing any to escape to the outside air. The outer shell was built from an ordinary truck muffler having 3" diameter inlet and exhaust ports. Steel grating was welded inside to support the glass wool and a spacer was built to separate the filters from each other and to allow removal of the filters when the test was finished. In testing there was some difficulty establishing the right amount of glass wool. Too little resulted in melting of the wool and too much blocked the flow. Another problem was that the wool became saturated with water if the outside temperature was below the dew point. The glass wool filter housing is shown in Figure 3.12. In the end these filters were not used.

The HEPA filter was mounted in the case shown in Figure 3.13A and B. Since exhaust water condensation was a problem a water trap was installed upstream of the filter. The trap was connected to the glass wool container (which was still in-line though not used) by copper tubing. The vacuum pump drew a flow rate of 0.8 gpm.

The engine was run for 15 minutes, this being enough time for radiation to collect on the filter if the level was indeed hazardous. Subsequent tests of the filter showed no radiation greater than background. Tests of the trapped condensed water also showed no radiation greater than background. Based on these results, it was judged safe to run the engine without diluting the exhaust.

3.2.9 System Environment

The dynamometer was rolled outside on rails where the noise of operation would not disturb everyone in the bullding (Figure 3.14). It was shielded from the elements by a canvas tent. The detector and oil reservoir remained inside the lab along with the dynamometer controller and other electronics.

3.3 Data Acquisition

The data aquisition system includes the detector (discussed earlier), and the Multi Channel Analyzer, which consists of the Amplifier, the Analog to Digital Converter, and the Digital Stabilizer.

3.3.1 The Amplifier

The amplifier takes poorly defined pulses from the preamplifier and smooths them into near gaussian shapes to ensure that the signals entering the ADC are consistent.

3.3.2 The Analog to Digital Converter (ADC)

The ADC takes the input voltage pulses from the amplifier and converts them to clean digital signals that the computer can read. An input of 0 to +10 volts is divided into a number of channels specified by the user. The higher the number of channels, the greater the resolution. For this study 8192 channels were used. The input pulses are placed into channels according to energy; higher energies pulses are placed in higher channels.

3.3.3 The Digital Stabilizer (DS)

The Digital Stabilizer receives signals from the ADC and ensures that the ADC places pulses of a particular energy in the same channel every time. While it does this automatically it needs information from the operator to do the job correctly. The operator needs to give the stabilizer two reference peak channels that it should stabilize about, one high energy and one low energy. If this is not done, the pulses that should be close to a particular peak energy channel will be sent to channels much further away, broading peaks or even creating false peaks.

3.3.4 The System 100 (S100) software

Signals from the detector are sent through the multi channel analyzer (MCA) to the personal computer. The S100 software enables data collection, display, and filing. Data is displayed on the screen with channels on the horizontal axis and number of counts on the vertical, allowing easy energy calibrations. S100 allows easy aquisition of peak areas off the main screen.

3.3.5 Microsampo

Microsampo is a software package designed to calculate accurately peak areas, activities, and efficiencies from data collected by System 100. This program has many flaws however and is very user unfriendly. Details of the operation are given in the manuals but an overview of its operation and discussion of some important points is given below.

General Operating Procedure

1) Input data files from the System 100
2) Program the energy calibration used for the S100 spectra
3) Perform a peak search - this tells Microsampo to go through the spectrum and identify all the peaks that are significantly above the level of background radiation.
4) Calibrate peak shapes. This is the calculation of shape parameters used to speed up the next step, peak fitting.
5) Fit peaks. this is the calculation of shape functions, based on parameters calculated previously, which enable the calculation of peak areas.

3.3.5.1 Shape Calibration

Shape calibration is the creation of shape parameters to speed up fitting. Shape functions, consisting of gaussian centers and exponential tails, are matched to a few good peaks (a good peak is one that has a gaussian shape). The parameters derived from these functions are peak width (cw), which is the standard deviation in channels of the gaussian; the lower tail parameter (cl), which is the distance in channels from the centroid to the point where the lower tail connects to the gaussian; and the upper tail parameter (ch), which is the distance from the centroid to the point where the high tail connects to the gaussian. The parameters derived from these good peaks are then used in the peak fitting process for all of the peaks.

Microsampo requires the user to go through the spectrum peak by peak, examine the agreement between function and actual peak shape, and either accept or reject the parameters derived from this match. If the match is not acceptable; the user can reject it, change some fitting options, and try a rematch. The only matching options are the high and low end of the match intervals. A good match looks like Figure 3.15. A match in which the interval should be widened is shown in Figure 3.16.

3.3.5.2 Peak Fitting

Peak fitting is the process of putting together the shape functions to approximate the actual peak shape and calculating the area of the peak. The computer calculates the peak areas by integrating under the shape function curves and subtracting the background continuum. Microsampo reports the peak area, area error, and the goodness of fit. The user has two options available to control how Microsampo draws the background continuum and two more to control how it puts the functions together. The continuum is drawn either linearly or parabolically, as shown in Figure 3.17A and B. The shape functions are fitted either linearly or nonlinearly. In the linear fit, the centroid of the peak is matched to the gaussian functions centroid and the functions are constructed from the match. Nonlinear fitting means that the cenroids are allowed to vary as the shape functions are put together. The user must choose the combination that produces the lowest error through a trial and error method. The combinations are summarized below:

1) linear continuum - linear fit

2) linear continuum - nonlinear fit

3) parabolic continuum - linear fit

4) parabolic continuum - nonlinear fit

Another important option is the interval width. After finding the fit-continuum combination for least errors, the errors can sometimes be reduced even further by manipulating the fitting interval width. Trial and error is required here but a little experience will show which peaks can be improved and which cannot.

Once all the peaks have been fit, a table of peak areas is produced. This peak fit report should be sent to the printer because peak fit results cannot be saved to disk. Once areas have been calculated, Sampo allows you to calculate efficiencies and activities, but its routines are very user unfriendly and not accurate. In fact, only the peak areas were used in any of the work for the present study.

3.3.5.3 Microsampo Problems

Many times during use of Sampo, and totally without warning or a pattern, the message "Insert write protect, hit any key to continue" will appear. If it happens consecutively, it means the program will crash after several more repetitions of the message. No reason for this has been discovered.

Another problem with Sampo is that peak fit results cannot be saved to disk for later use or modification. This means that to rexamine the data set the peaks will have to be fit again, requiring an additional hour of time. This lack of proper documentation is one of Sampo's greatest flaws.

3.4 Calibrations

The activity of any sample measured by the detector is given by the formula:

$$\text{Activity} = \frac{\text{peak area}}{(\text{livetime})(\text{branching ratio})(\text{efficiency})} .$$

The peak areas and livetimes (livetime being the time spent counting radiaton) are readily measured, the branching ratios are known, but the efficiency is not. As discussed in appendix C, to get an efficiency curve for a set position relative to the detector a known source must be placed in this position and measured. The ratio of the measured intensities to the actual (known) values is the efficiency at that position. For this study, accurate counts of the piston ring and oil had to be made repeatedly. To make this possible, efficiency curves were generated for fixed reference positions near the engine block and oil reservoir. An efficiency curve was also generated for a general reference position where the ring could be counted before and after the test.

3.4.1 Oil Reservoir Calibration

Before the activity in the oil can be calculated, an efficiency curve must exist for the detector in its fixed position within the reservoir. This means that a known source of radiation must be placed within the reservoir and measured. Only a source in a water solution could be put in the reservoir and completely removed without contaminating the reservoir. $ThCl_4$ was chosen because it is a naturally occurring radioactive substance, it has well known peaks, it is available in a water soluble powder form that had a low enough activity to be shipped as a non radioactive substance.

The calibration procedure is outlined below:

1) Count the $ThCl_4$ in a fixed position, called position A, near the detector while it is in powder form and as close to a point source shape as possible.

2) Measure a known source at position A to create an efficiency curve. Use this curve to calculate the $ThCl_4$'s activity.

3) Mix the $ThCl_4$ in a water solution and put it in the reservoir. Count the reservoir.

Step 1: 5 mg of $ThCl_4$ in a glass bottle was placed 25 cm away from the detector on the detector centerline. The distance was measured from the detector to the powder inside the bottle. This was called position A. The $ThCl_4$ was counted.

Step 2: The known point source (a mixed standard containing the nuclides antimony 125, tellurium 125, europium 154 and 155), was placed at position A. The source was counted.

Step 3: After some experimentation a vacuum pump was used to draw air out of the reservoir resulting in water being drawn in to replace the air. The line from the reservoir to the pump was long and coiled so that when water was observed exiting the reservoir there would be time to shut off the pump before the water reached the pump. Experimentation showed that if the water in the beaker dropped to a level near that of the end of the intake hose air would enter the lines. Thus a large enough volume of water was used so that when the reservoir was filled and the pump was shut off, the level of water in the beaker was higher than the hose end. The reservoir volume is 1260 ml.

A white sheet was placed over the lab table. 17 ml of thcl4 was placed in a 1300 ml of water. To this 3 ml of food coloring was added so that any spills could be easily located on the white sheet. The total volume of solution was 1320 ml. The vacuum pump was used to get the solution into the reservoir. Once the reservoir was full the small amount of solution still in the lines was put back in the beaker. The volume fraction of thcl4 solution in the reservoir to the total volume of solution was .9545 ± 4.8%. The reservoir was then counted.

The efficiency curve shown in Figure 3.18, which was generated using the mixed point source, was used to obtain the activity of the thcl4. The curve shown in Figure 3.19 is the efficiency curve for the solution in the reservoir itself.

3.4.2 Piston Ring Check In

To obtain a measurement of the initial piston ring activity a special platform was built. This platform enables exact repositioning of the piston ring every time a measurement is made, such as before and after the testing. This position is called position R. Three known sources were in position R. The sources were a combination europium standard (the same one used for the coil calibration), a steel foil activated with co-56 that was supplied with the piston ring from KFK, and a sample of Eu-152. These sources were then counted to get an efficiency curve for this position. The curve is shown in Figure 3.20. The rings activity was measured to be 7.5 microcuries.

3.4.3 Cylinder Calibration

For the direct radiation measurements necessary in the Marker Method an efficiency calibration was necessary in the cylinder of the engine. To this end two point sources were placed at the same position in the cylinder and measured. Because of the error in the placement of the sources the resulting effeciency curves were significantly different from each other. This was becuase the sources were approximately one inch away from the detector when being measured. At this distance even very small innacuracies in the positioning of sources can have a very large effect on efficiency. Because there was no way to reposition the sources with any greater accuracy the tests were run without an efficiency calibration for this position. The relative intensities are all that is necessary for the wear calculations in the marker method, and these were measured directly.

CHAPTER 4

THE EXPERIMENT

4.1 Calculation of Ring Wear

The depth calibration profile shown in Figure 4.1 was provided with the ring from KFK. The relative intensity is the number of gamma photons per second given off by the ring after a test period divided by the amount of gamma photons given off before the test period. One way to calculate this is to make a direct count of the piston ring activity before a given test run, getting A_{before}, then count the ring after the test run, getting A_{after}. The relative intensity is then:

$$\text{Relative intensity} = A_{after} / A_{before} \qquad (4.1)$$

Wear, in micrometers, is then calculated from the line fit to the depth calibration:

$$\text{Wear} = 54.5*(1 - \text{Relative Intensity}) \qquad (4.2)$$

Another way to calculate the relative intensity is from the amount of radiation in the oil. The relative intensity after the nth test run is given by:

$$\text{Relative Intensity} = [A_{ring} - A_{oil}(n)] / [A_{ring} - A_{oil}(n-1)] \qquad (4.3)$$

Equation 4.2 is then used to calculate the wear. Note that in this case A_{ring} is the original activity of the ring decay adjusted to the activity it had at the time of the oil count:

$$A_{ring} = A_o * \exp(\ln2*\text{decay time} / \text{halflife}) \quad (4.4)$$

A_{oil} is the activity counted in the oil reservoir multiplied by the ratio of total oil volume to reservoir volume:

$$A_{oil} = (\text{total volume} / \text{reservoir volume})(A_{reservoir}) \quad (4.5)$$

It is assumed that the volume ratio is constant. This may not always be the case due to changes in oil temperature, oil losses, and cavitation induced air bubbles. The error in the wear is calculated as follows:

$$\text{Wear error} = [\, 2*(A_{ring}\ \text{error})^2 + (A_{oil}(n)\ \text{error})^2 + (A_{oil}(n-1)\ \text{error})^2 \,]^{1/2} \quad (4.6)$$

Where the A_{oil} error is:

$$A_{oil}\ \text{error} = [\, (\text{volume ratio error})^2 + (\text{oil reservoir activity error})^2 \,]^{1/2} \quad (4.7)$$

Calculation of wear rates is then just the nth measurement of wear divided by the length of the nth test run:

$$\text{Wear rate} = \text{wear}(n) / \text{Run time}(n) \tag{4.8}$$

Assuming no error in the measurement of time the error in the wear rate is equal to the error in the wear.

4.2 The Procedure

Since the wear rates in the test engine were completely unknown before the study, the procedure had to take into account the possibility that all of the radiation could be worn off in a very short time, even a matter of minutes. To this end, the tests were started at low speed and low load to minimize wear. Whenever counts of the piston ring were necessary, the detector was set on a steel platform bolted to the engine stand. This platform ensured that the detector centerline was at the same height as the piston ring when the piston was at top dead center. The platform also allowed the detector to be held close to the block for high efficiency. To count the oil, the detector was placed in the reservoir-detector stand described earlier.

The test procedure is outlined below:

1) Run the engine at set speed and load for a set time.

2) Stop engine, count the ring.

3) Pump the oil into the reservoir and count the oil.

Note that the oil pump was not run continuously. There were two reasons for this. The first was that the pump had begun to leak. Replacing the pump was tried but no pump that matched the existing hose size could be found within the time constraints of the study. The second reason was that if the pump and engine were run simultaneously the oil activity would be increasing while it was being counted. This was due to the fact that the time for the detector to count the low activity in the oil was initially very large. The data from the oil was used to calculate wear rates during the test in order to determine at what speed and load levels the engine should be run. Figure 4.2 shows the power levels the engine was run at.

The engine was run at its stock compression ratio for the first 23 hours of the test. Afterwards, the compression ratio was increased from 7.6 to 9.5 in the hopes of increasing the wear rate. The engine was then run for 18 more hours at the same power level to see the effect of this modification. Next, a friction reducing oil additive was added to the oil. Immediately after this addition, the engine head cracked, therefor no data as to the effect of the additive was obtained. Then engine was then motored for 7 hours to see the effect of very low loads. The data from the motored tests seem to be flawed, however, because during a move of the test equipment to a new site; a wire in the detector broke, and the reservoir suffered repositoning.

4.3 Results

Figure 4.3 is a plot of the engine wear rates vs. cumulative run time. In the first hour of the test, data was taken at 15 minute intervals; and a clear break in period of high wear rates was observed. After this peak, the wear rates stayed fairly constant despite variations in engine power and speed. the Another break-in period is evident when the compression ratio was raised. This break-in did not reach the high wear rates of the first peak, however. The wear rates steady out for about 18 hours after the second break-in period, during which time the power is held constant. After this period, the head cracked and motored tests were begun. The data for the motored tests is flawed, however, because of a broken detector wire and movement of the oil reservoir from its reference position.

CHAPTER 5

SUMMARY & CONCLUSIONS

Parameters affecting the calculation of wear are listed below.

1) Method of measuring radiation

   A) The marker method requires much less time to measure radiation with less than 5% peak area error than the tracer method does. The marker method is unable to measure a difference in the level of radiation that is smaller than approximately 1%. This results in more time being required, compared to the tracer method, to estimate wear.

   B) The tracer method was used to detect the wear rates in this study while the marker method was unable to detect any wear. This was becuase the total radiation worn into the oil was below 1% of the initial radiation in the ring. Thus, while the tracer method requires more instrumentation, it is more sensitive than the marker method and estimates of wear rates can be made with the very first measurement. Typical counting times to reduce errors to 5% for the tracer method, under the present test conditions, are approximately 50 minutes.

2) Length of test runs: Shorter run lengths will allow a better estimate of the shape of the wear rate curve. Every test run, however, requires a 50 minute reservoir measurement, so for short run lengths most of the time will be spent measuring rather than running.

3) Precision of detector positioning: Since the efficiency curves necessary for activity (and thus wear) calculations are generated for only one fixed position relative to the detector, the source of radiation must be in the same position every time a measurement is made. The detector is extremely sensitive to sample to sample variations in

this position. At a distance of 1 inch from the detector, a variation in the reference position of 1/8 inch is enough to completely invalidate the efficiency curve.

4) Oil volume: The accuracy of the tracer method depends on the accuracy in the measurement of the total oil volume. This volume can change over time due to the burning of oil by the engine and oil leaks in the lines. Although the reservoir volume is constant the volume of oil in it is not, due to the presence of air bubbles. The mass of oil in the reservoir will not always be the same even if the volume is constant due to temperature induced density variations.

5) Intrinsic detector parameters:

   A) The detector has been known to shut down, for unknown reasons, during a measurement. When this happens, the software clock does not stop, meaning that a greater counting time is indicated than actually happened. A comparison of spectrum background peaks can be used to check for detector shutdown. Background peaks from data taken in the same position should have the same intensity. Large variations in the intensity may indicate detector shutdown.

   B) Any warming of the detector will reduce its resolution. There is no indicator that this is happening, however, so care must be taken to keep the detector cool. The effective dewar holding time is 30 hours so conscientious filling is necessary.

6) Test Engine: Very small loads had large effects on engine speed, severely limiting the range of loads and power that could be studied. For friction and wear testing of diesel and gasoline powered automotive engines the radiotracer technique would appear to be ideal.

7) No hazard exists from the exhaust given off by the engine run in this study. The final activity of the oil is below the legal limit, which is 2

microcuries per gram, set by the department of Transportation for disposal as a radioactive substance. The thorium compound is a naturally occurring radioactive substance and thus is not regulated.

CHAPTER 6

RECOMMENDATIONS

1) Detector:

   A) The detector must always remain cool. It must not be placed too close to the engine block or allowed to be in the reservoir unless the cooling system is on.

   B) Detector cables should have crimp-on BNC connectors. The screw-on variety come loose and cause short-circuits. Detector cables should not be looped because this will cause system noise.

   C) A pulser should be used to double check the detectors indicated livetimes.

   D) A more precise method of securing the detector in position should be used. This method should eliminate the metal straps that hold the detector to its base, because these have a small amount of play in them.

2) Environment: A test cell is needed to shield the experiment from wind and rain. A dedicated cell is needed to conduct wear tests of this type.

3) Sources should be tested before being used to generate efficiency curves.

4) Oil System:

   A) Very careful measurement of the system oil should be made using a graduated cylinder or similar measuring device. A means of measuring the oil volume while tests are in progress should be developed. This method should be more accurate than the dipstick.

B) The oil system as a whole, (the engine, the pump, the reservoir, and the oil lines), should be calibrated by using a radioactive source to quantify the effect of air bubbles on the volume calculations. The radiation measured in the reservoir divided by the total radiation should ideally be equal to the ratio of reservoir volume to the total system volume. The amount by which these numbers differ will indicate the errors in the process, much of which may be due to air bubbles.

C) Minimizing the number of joints in the plumbing and soldering all joints is a necessity.

5) A test engine that was designed to operate at a wide range of speeds and loads should be used .

6) New software must be purchased or written that meets the following criteria:

A) Must be able to back up and print out all data and plots.

B) Must be able to communicate with each other, if multiple codes are used.

C) Must be able to calculate wear rates directly from spectral data.

7) Once the tests are started there should be no shutdown of the detector or movement of the oil reservoir.

8) One addition that should be made is a plexiglass shield to cover the engine assembly. This would keep oil from being sprayed across the room if the oil hose burns through where it is in contact with the engine.

REFERENCES

LIST OF REFERENCES

1. R. Evans.."Radioisotope Methods for measuring Engine Wear: A Thin Layer Activation Method for the Measurement of Cam Follower Wear and its Comparison with a Neutron Activation Method". Shell Research Ltd., Thornton Research Centre, Great Britian, Nov 26, 1979

2. F.H. Kinsella and T.H. Childs.."A Study of Wear in the Friction Cutting of Cast Iron Using Thin Layer Activation", Wear, 66 (1981), 241-255

3. S.G. Fritz and G.R.Cataldi "In Situ Piston Ring Wear Measurements in a Medium Speed Diesel Engine", Lubrication Engineering, Vol 46,6, 365-370

4. Eric W. Schneider and Daniel H. Blossfeld.. "Effect of Speed and Power Output on Piston Ring Wear in a Diesel Engine", International Congress and Exposition, Detroit, MI, February 29- March 4, 1988, SAE 880672

5. S.A.Elbakr, I.J. Van Heerden, W.J. McDonald, G.C.Neilson, "Measurements of Nuetron Angular Distribution From the 7li(p,n)7Be Reaction". Nuclear Instruments and Methods 105, (1972) 519-523, North Holland Publishing Co.

6. Burkhardt T., McHarris W., Lloyd J., Rachel T., Schock H., Grummon D, Shalek R, Ronningen R, Mallory M, "Developments in High Energy Ion Implantation For Wear Studies", Michigan State University Status Report, MSUERL-90-5, 1990

7. Personal Communication

8. Ziegler J.F., Biersack J.D., Littmark A., "The Stopping Power of Ions in Solids", Pergamon Press Inc, Maxwell House, Fairview Park, Elmsford, N.Y. 10523 USA

9. EG&G Ortec, "Quick List of Nuclear Decay", Academic Press

10. Lindeburg M. Engineer in Training Review Manual, Sixth Edition, Professional Publications, Inc, Belmont, CA 94002

11. Bevington P.R, "Data Reduction and Error Analysis for the Physical Sciences", McGraw Hill Book Company

APPENDICES

APPENDIX A

ERROR ANALYSIS

Statistical uncertianties arise from counting a number of events (such as emission of gamma photons) per unit time interval. The uncertianty is not due to imprecision in measuring the time interval or inexactness in counting the number, but due to the fact that the number of events fluctuate randomly from sample to sample. The uncertainty in counting a number of events per unit time interval is given by:

$$du/u = N^{1/2} / N,$$

where N is the number of events. This formula is used by the computer software to calculate the peak area error.

Other uncertainties come from tabulated values of branching ratios, reference values of calibration sources, and almost every measurement that is made. The propagation of these uncertainties is very important when determining wear rates. The following equations show the general form of error propagation in algebraic equations.

$$x = au \pm bv : \quad \sigma_x^2 / x^2 = a^2\sigma_u^2 + b^2\sigma_v^2 + 2ab\sigma_{uv}^2 \qquad \text{(A.1)}$$

$$x = \pm auv : \quad \sigma_x^2 / x^2 = \sigma_u^2 / u^2 + \sigma_v^2 / v^2 + 2\sigma_{uv}^2 / uv \qquad \text{(A.2)}$$

$$x = \pm au / v : \quad \sigma_x^2 / x^2 = \sigma_u^2 / u^2 + \sigma_v^2 / v^2 - 2\sigma_{uv}^2 / uv \qquad \text{(A.3)}$$

For the present calculations second order terms can be neglected. Thus the activity and activity error is calculated by the following equations:

$$\text{Activity} = \frac{\text{peak area}}{\text{(livetime)(branching ratio)(efficiency)}} , \qquad \text{(A.4)}$$

$$\text{Activity error} = [\,(\text{area error})^2 + (\text{efficiency error})^2]^{1/2} \qquad \text{(A.5)}$$

where the error in livetime and the branching ratios have been neglected as they are very small compared to the other errors. Since it is necessary to average activity values the following formula must be used to weight the average by the individual activity errors:

$$x = \Sigma(x_i / \sigma_i^2) / \Sigma(1 / \sigma_i^2), \qquad \text{(A.6)}$$

where x_i is the individual measurement, and σ_i is the individual measurement error. The uncertainty in this mean is given by:

$$\sigma_\eta^2 = 1 / \Sigma(1 / \sigma_i^2). \qquad \text{(A.7)}$$

APPENDIX B

PRODUCTION OF 7BE IONS FROM A 7LI BEAM AND A POLYETHYLENE TARGET

The Michigan State University National Superconducting Cyclotron is studying methods of producing 7be ions for wear studies. These ions would be implanted into components whose wear properties are being studied using the radiotracer or radiomarker method. This ion implantation technique would replace the presently used surface layer activation technique that can only be used on materials with atomic number greater than 24. The ability to do ion implantation on campus would greatly reduce the costs of wear studies and eliminate all the hazard and paperwork of shipping radioactive components overseas.

One reaction used to produce 7be ions is:

$$p(7Li,\ 7Be)n \tag{B.1}$$

Figure B.1 shows the set-up used to test this reactions production efficiency. The 7Li beam produces 7Be ions when it strikes the polyethylene targets. The 7Be ions have momentum in the direction of the 7Li beam so a stack of aluminum foils is needed to stop them. The number and distribution of the 7Be ions in the aluminum tells us how many ions were produced and their energies. This was only true, however, if no 7Be ions were produced by the 7Li beam striking the aluminum foils on its way through. To test this possibility a control stack of aluminum foils were struck with the 7Li beam and counted for any traces of 7Be.

The testing procedure is as follows:

1) An efficiency calibration is done for the position where the foils will be counted, called position 1.

2) A count is made of each stack (stack 1 consisting of the

polyethylene targets and 15 Al foils, stack 2 consisting of the second 15 foils)

3) Stack 1 was disassembled and each foil counted separately, the foils being mounted on cardboard sheets.

4) Stack 2 was disassembled and each foil counted separately.

Two sources of eu-152 were used to get the efficiency calibration curve for this test. One, the strong source, had an activity of 14.5 microcuries, while the other, the weak source, had an activity that was unknown. To detect the small amount of beryllium in the foils they had to be placed close to the detector to reduce the errors. The strong source however could not be placed close to the detector because it would cause a great deal of deadtime in the electronics. To get around this, the strong source was used to get an efficiency curve at a position further away from the detector, position 2, enabling the calculation of the activity of the weaker source. Once the activity of the weaker source was known it was placed in position 1, the position very near the detector, and used to generate an efficiency curve there. These two curve are shown in Figures B.2 and B.3.

The table below shows the data taken during the foil counts. This data was used to calculate the distribution of 7Be ions in the aluminum foils, this relation being plotted in Figure B.4. The data was also used to generate a depth calibration plot of the type received with the piston ring, as shown in Figure B.5.

APPENDIX C

EXAMPLE CALCULATION OF EFFICIENCY AND ACTIVITIES

As stated before the total efficiency of the detector is given by:

$$\text{Total Efficiency} = \frac{\text{number of photons striking the detector}}{\text{number of photons emitted by the source}} \quad (C.1)$$

The total efficiency is the product of the geometric efficiency, which is given by:

$$\text{Geometric Efficiency} = \frac{\text{number of rays striking the detector}}{\text{number of rays emitted by the source}} \quad (C.2)$$

and the intrinsic efficiency, which is given by:

$$\text{Intrinsic Efficiency} = \frac{\text{number of signals generated by the detector}}{\text{number of rays striking the detector}} \quad (C.3)$$

The geometric efficiency is inversly proportional to the distance between the detector and source. Because less rays strike the detector when it is further away from the source, as shown in Figure C.1. When the gamma ray detector is struck by a photon, it gives off a current pulse called a signal. The intrinsic efficiency reflects the fact that not every photon that strikes the detector causes a signal to be generated. In fact lower energy photons have a greater chance of generating a signal than do higher energy photons. An efficiency curve must be generated that shows efficiency as a function of energy. This curve would be valid for only one set position (one fixed distance between source and detector) due to the geometric efficiency. Such a curve is shown in Figure C.2 Above approximately 200 keV, there is a nearly linear relationship between the log of the energy and the log of the efficiency.

Before any efficiency curves can be generated the computer must be able to distinguish between the energies of the signals it is receiving. Figure C.3 shows a simple analogy of how the computer receives and stores signals. Pictured is a coin bank. Coins roll down the slot and fall into the first bin that is large enough to hold them. If it is American currency being put into the bank then one can easily deduce which slot holds which coins because the sizes of dimes, nickels, etc., are well known. If however an unknown currency is put in, then the value of the coins in any particular bin is unknown, only their size relative to one another is known from the bins they fall into. The multi-channel analyzer (MCA) and computer function in a similar manner with the signals generated by the detector. Signals are received by the MCA and put in bins called channels. The signals generated by the higher energy photons, like the larger coins, fall into channels further to the right than the signals generated by the lower energy photons. So, although the signals are sorted by energy, the computer cannot label any particular channel as any particular energy. What is needed to identify the energies is called an energy calibration.

Before energy-channel calibration can be discussed, however, an important difference between the bank analogy and the computer system must be recognized. In the bank the number of coins in any bin is known exactly. In the computer, however, the placement of signals into the right channels is not completely accurate. In fact, the signals become arrayed in a gaussian pattern about the channel that corresponds to their energy. To get the total number of signals for one energy, a count must be made of the signals in the channel that corresponds to that peak energy, and in the channels around it. Figure C.4 shows a gaussian shaped peak, channels being on the horizontal axis and number of counts on the vertical. Integrating under the gaussian curve gives the peak area, which is the

error in

of cou

lower

counts

corresp

known

exampl

Figure

backgr

peaks

within

clear f

table;

of th

relati

acc

ide

pro

pa

ca

be

ac

sec

exam

inform

is the total number of counts, N, above background at that energy. The error in this area is approximately equal to the square root of the number of counts divided by the number of counts, so the greater the area the lower the error. To minimize errors it is then necessary to have many counts and thus long counting times.

$$\text{Area error} = N_{1/2} / N \tag{C.4}$$

To enable the computer to recognize which channels correspond to which energy an energy calibration must be performed. A known source is placed in front of the detector and measured. An example spectrum taken from a count of europium 152 is shown below in Figure C.5. Examination of the spectrum shows several peaks above the background. The specific energies at which europium has its strongest peaks must be determined from tabulated data and located by their size within the spectrum shown. Then, since the channels of these peaks are clear from the spectrum, and their energies have been determined from a table; linear interpolation between these channels allows the calculation of the energies of every other channel. Once this energy-channel relationship is known, the identification of any unknown source is easily accomplished. The energies of the biggest peaks in the spectrum are identified and compared to tabulated values to determine what nuclide produces them. Recall every nuclide has a characteristic peak energy pattern.

Once the channel-energy relationship is known, an efficiency curve can be generated. To generate an efficiency curve, a known source must be measured at some fixed position from the detector. Since the source activity and identity are known, the exact number of gamma photons per second (intensitiy) it emits at its characteristic energies is known. For example, if our known source is europium 152 we have the following information:

Table C.1 Branching Ratios of Europium 152

Energies [keV]	Branching Ratio [Gammas per 100 decays]
121.78	.284
344.28	29.58
1112	13.56
1408	20.85

Since its activity is known, for example in this case 9 microcuries (333000 d.p.s.), intensities can be calculated:

intensity (gammas per second) = activity * branching ratio

Table C.2 Known Intensities

Energies [keV]	Intensity [Gammas per second]
121.78	94572
344.28	98501
1112	45155
1408	69430

If the source is counted for 1000, seconds the following data might be the result:

Table C.3 Measured Intensities

Energies [keV]	Intensity [Gammas per second]
121.78	260410
344.28	199550
1112	54280
1408	72087

Dividing the peak areas by the livetime gives the number of photons counted per second at each energy. The livetime in this case was 1000 seconds. The total efficiency is then the number of counts per second divided by the number of gamma photons per second.

Efficiency = (counts / second) / (photons / second)

Table C.4 Efficiencies

Energies [keV]	Efficiency [counts per photon]
121.78	.002754
344.28	.002026
1112	.001202
1408	.001038

A log-log plot of this is shown in Figure C.6.

The error in the efficiencies is calculated using the equation

$$\text{Efficiency error} = [\ (\text{area error})^2 + (\text{activity error})^2 + (\text{branching ratio error})^2\ ]^{1/2}$$

The area error is given by the computer with the peak area. The activity error is the uncertainty of the source activity. The errors in the branching ratios are typically tabulated, but for the most part they are so small that they can be neglected.

Once the errors in the efficiencies are known, a line is fit through the points, the fit being weighted by the errors. A computer routine given in Reference [1] is used to do this. The fit allows the calculation of efficiencies for energies that are between those of the europium peaks. The fit error is derived from the efficiency errors.

Once the efficiency curve is known for some detector position, it can be used it find the activity of an unknown source placed in this position. The activity is given by the equation below

$$\text{Activity} = \frac{\text{peak area}}{(\text{livetime})(\text{branching ratio})(\text{efficiency})}$$

Livetime is the amount of time the computer actually spent counting. It is real time minus the time the computer shuts down to process signals. This shutdown time is called the deadtime. Livetime = realtime - deadtime. Dividing by the total efficiency gives the total number of gamma photons, called intensities, emitted by the source at that energy. Dividing by the branching ratio, which is the intensities per 100 disintegrations for this energy, the total number of disintegrations per second is found. This is the measurement of activity. This activity calculation will be done for the major peaks in a spectrum and the error weighted mean of the results will be the activity, as shown in chapter 2.

Example: Using a source of Eu-152, an energy and efficiency calibration is created as shown in Figure. Next, the unknown source is placed in the position of known efficiency and is counted for 1000 sec, resulting in the spectrum shown in Figure C.7 below. By comparing the energies of the four largest peaks in the spectrum below, (846, 1037, 1238, 1771 keV), with tabulated values, one can identify the nuclide as Co-56. It has the following branching ratios (from tables) and peak areas (from the count data):

Table C.5 Peak Areas

Energies [keV]	Branching Ratio [gammas /100 decays]	Peak Areas [counts]	Area error [% error]
846	.9996	121590	0.3
1037	.1016	15613	0.9
1238	.6697	63573	0.4
1771	.1551	11053	1.0

The efficiency of the detector at these energies is then calculated from the line fit to the efficiency curve on Figure C.6.

Table C.6 Efficiencies at Cobalt 56 Energies

Energies [keV]	Efficiency [counts per photon]	Efficiency Error [% error]
846	.0009099	0.2
1037	.0008356	0.2
1238	.000776	0.2
1771	.00066815	0.2

From here the activity can be calculated from each peak area

$$\text{Activity} = \frac{\text{peak area}}{(\text{livetime})(\text{branching ratio})(\text{efficiency})}$$

$$\text{Activity error} = [\ (\text{area error})^2 + (\text{efficiency error})^2]^{1/2}$$

This formula for activity error assumes negligible error in the branching ratio and livetime.

So the activities and errors are

Table C.7 Activities of Cobalt 56

Energies [keV]	Activity [Decays per second]	Activity Error [% error]
846	133683	0.36
1037	183905	0.92
1238	122329	0.45
1771	106658	1.02

Ideally all these values would be the actual activity and thus all the same. As it is, an error weighted mean of the above values will approximate the actual activity:

$$\text{Mean activity} = \frac{\Sigma(\text{activity}_i\ /\ \text{activity error}_i^{\,2})}{\Sigma(1\ /\ \text{activity error}_i^{\,2})}$$

$$\text{Mean activity error} = \frac{1}{[\,\Sigma(\,1\,/\,\text{activity error}_i^{\,2}\,)]^{1/2}}$$

FIGURES

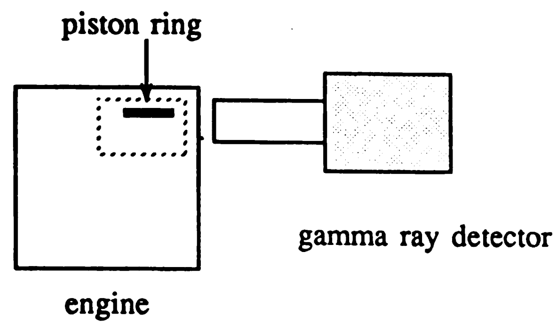

Figure 2.1A The Marker Method

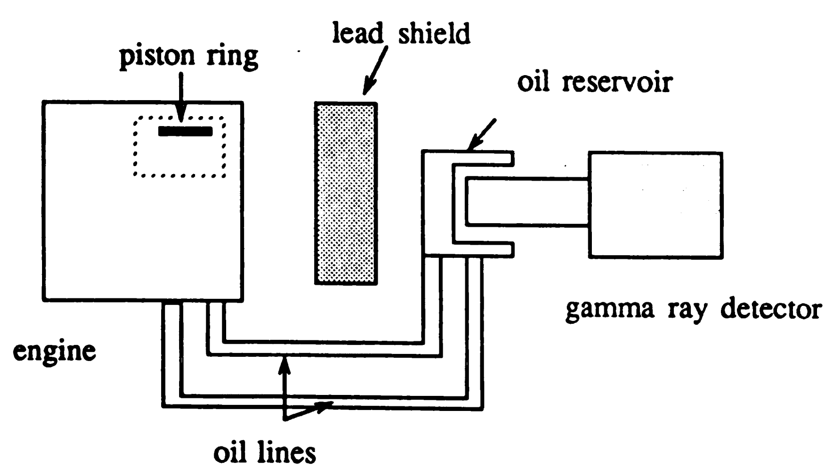

Figure 2.1B The Tracer Method

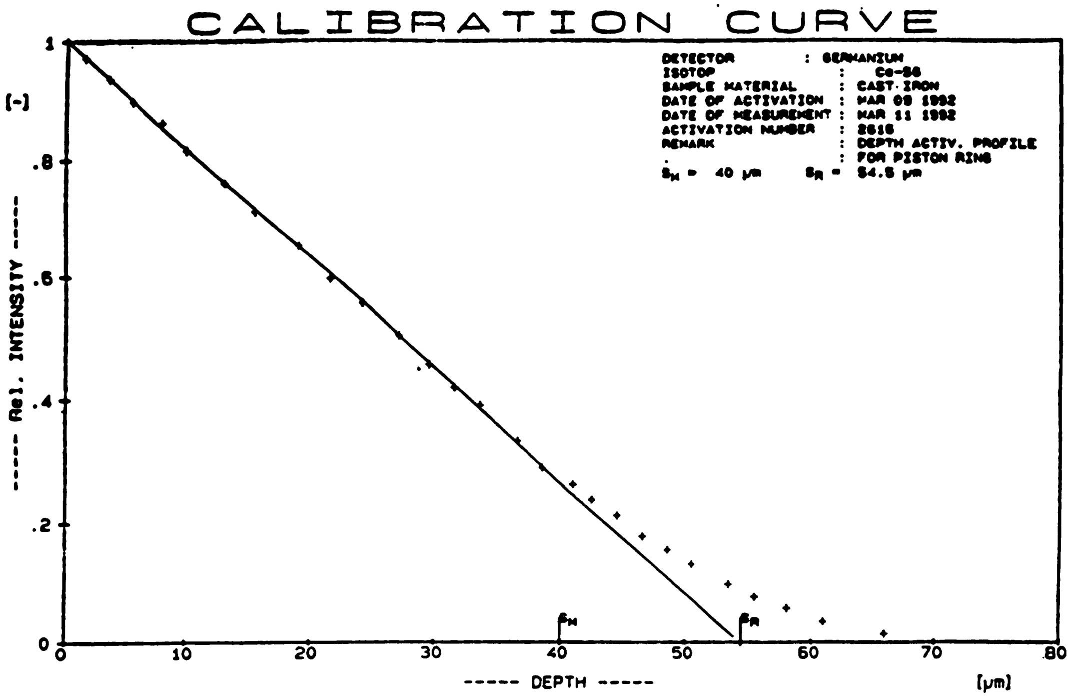

Figure 2.2 Depth Calibration Curve

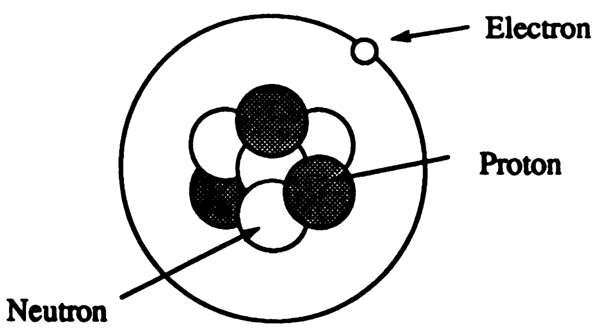

Figure 2.3 The Atom

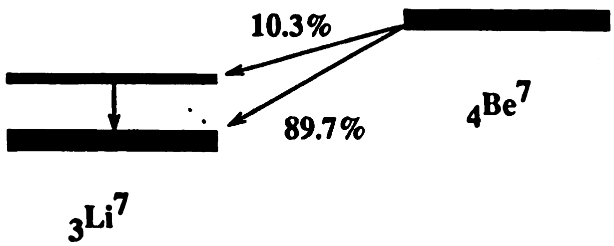

Figure 2.4 Be^7 Decay Path

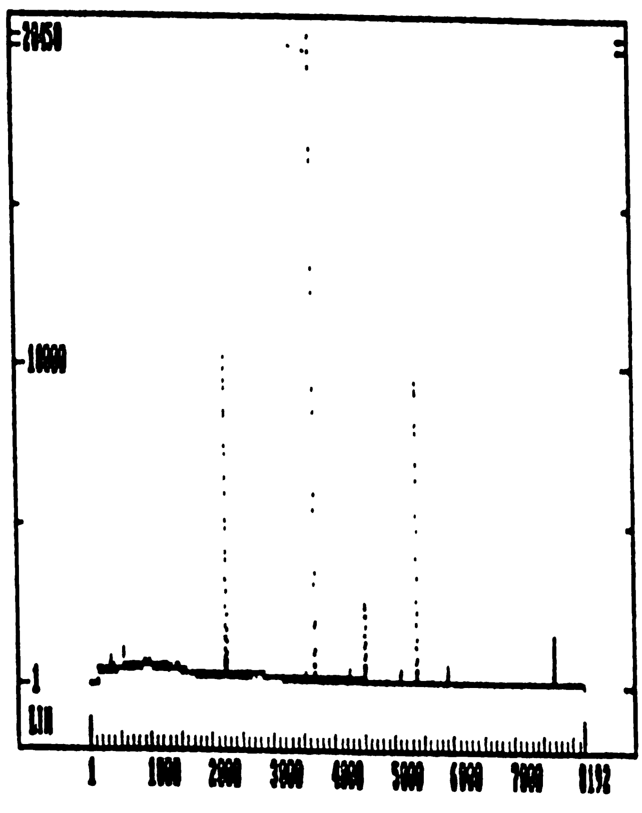

Figure 2.5 Cobalt-56 Spectrum

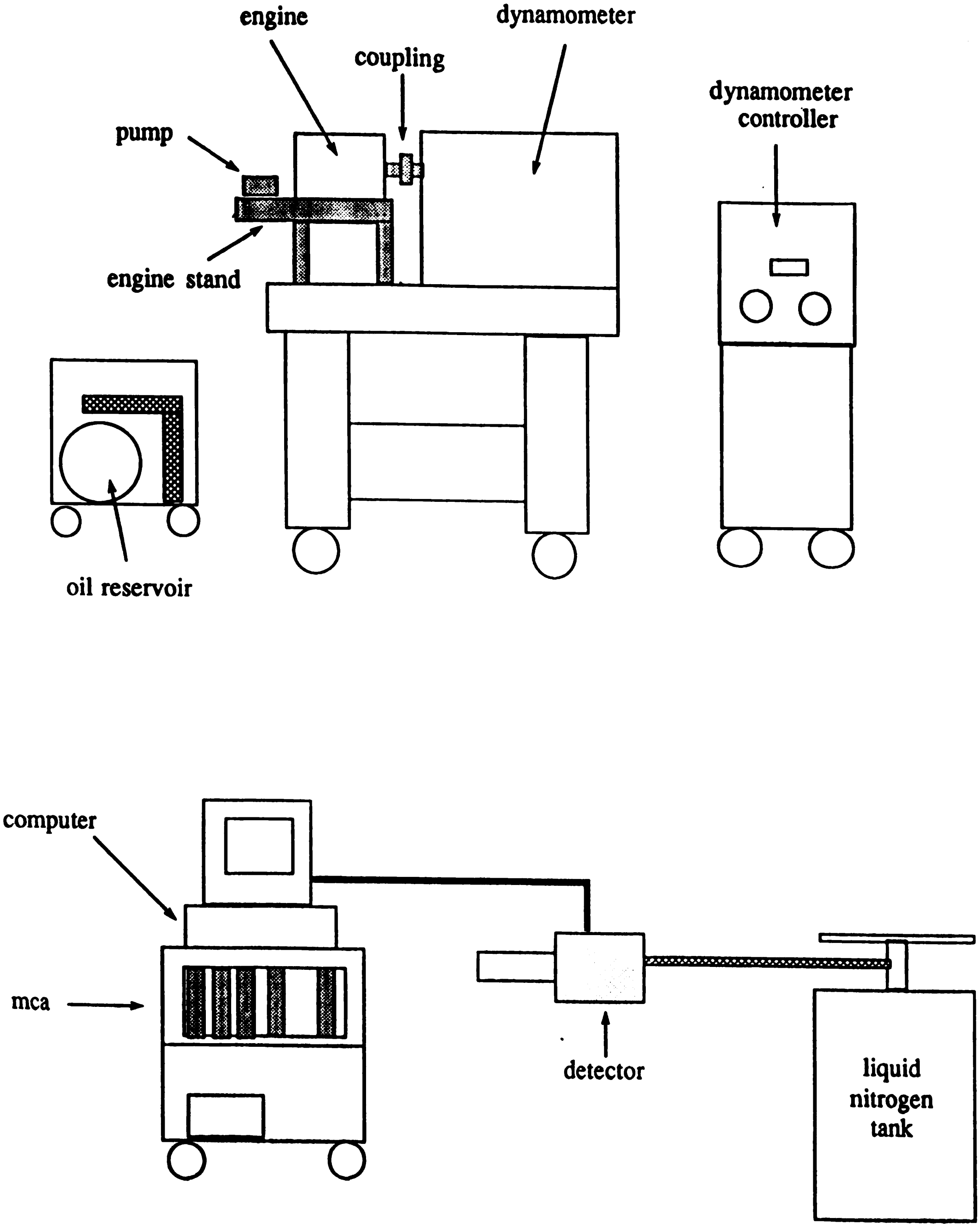

Figure 3.1 System Components

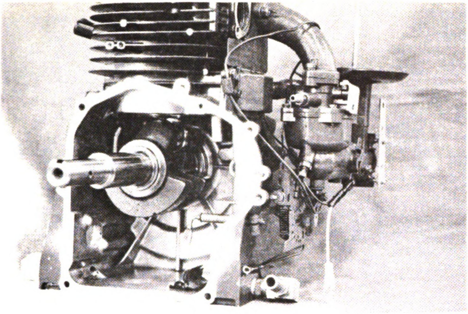

Figure 3.2 Engine Block

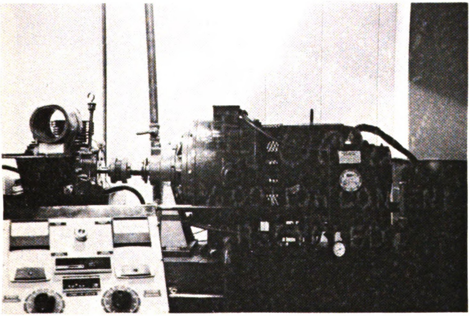

Figure 3.3 Dynamometer

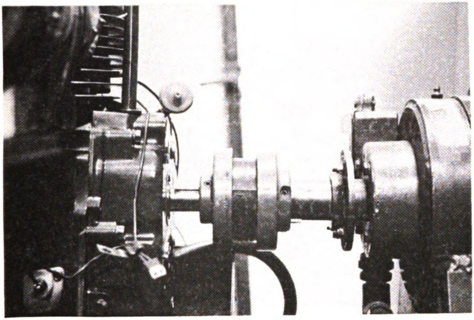

Figure 3.4 Coupling

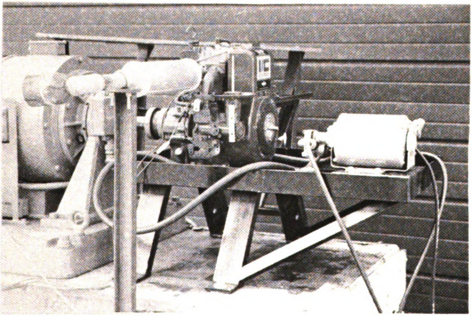

Figure 3.5 Engine Stand

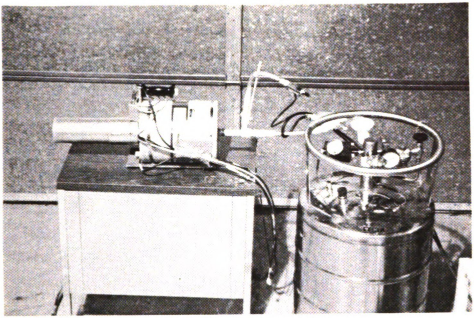

Figure 3.6 Gamma Ray Detector

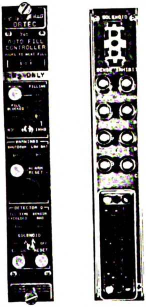

Figure 3.7 Auto Fill Controller

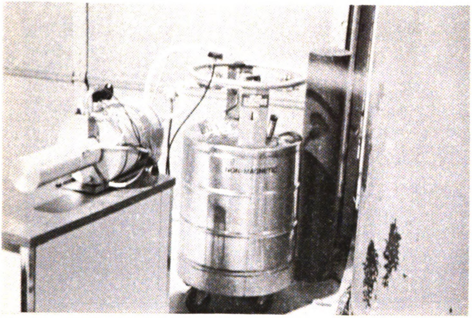

Figure 3.8A Detector Filling

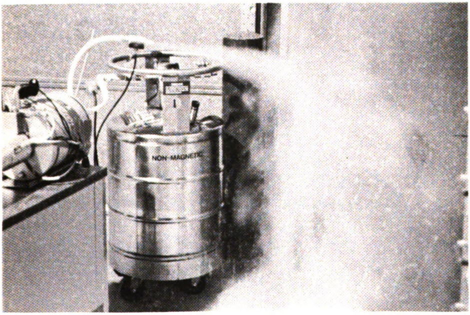

Figure 3.8B Detector Full

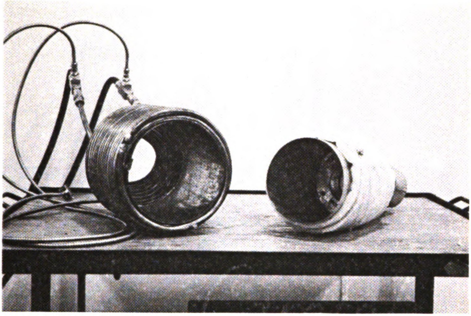

Figure 3.9 Oil Reservoir

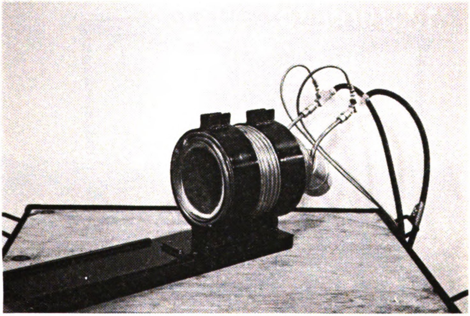

Figure 3.10 Reservoir-Detector Stand

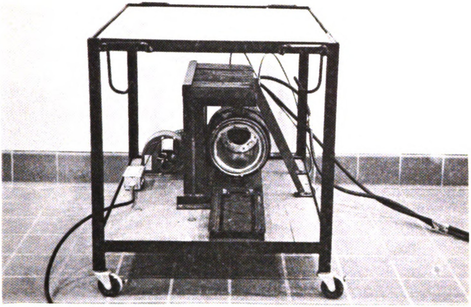

Figure 3.11A Reservoir Platform

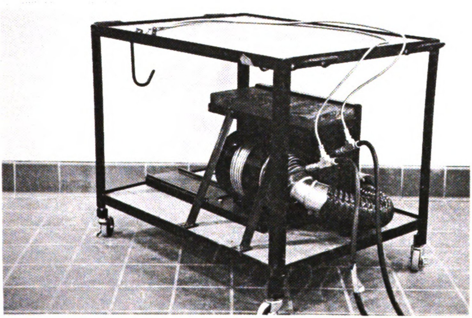

Figure 3.11B Reservoir Platform

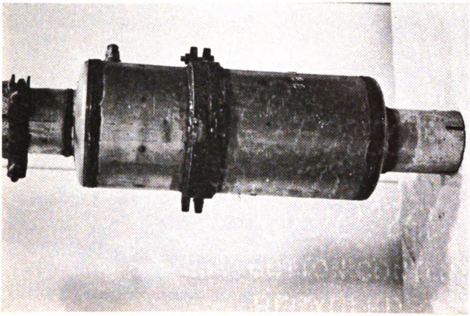

Figure 3.12 Glass Wool Filter Housing

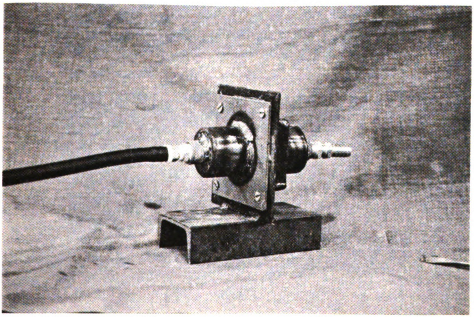

Figure 3.13A HEPA Filter Housing

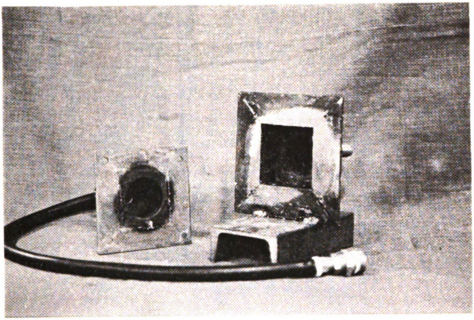

Figure 3.13B HEPA Filter Housing

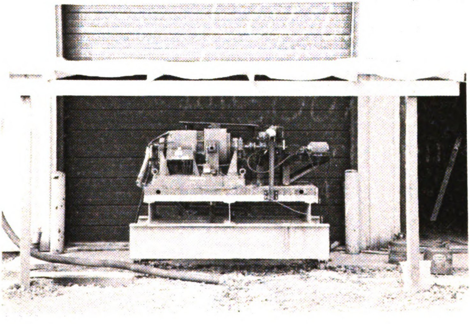

Figure 3.14 Test Set-Up

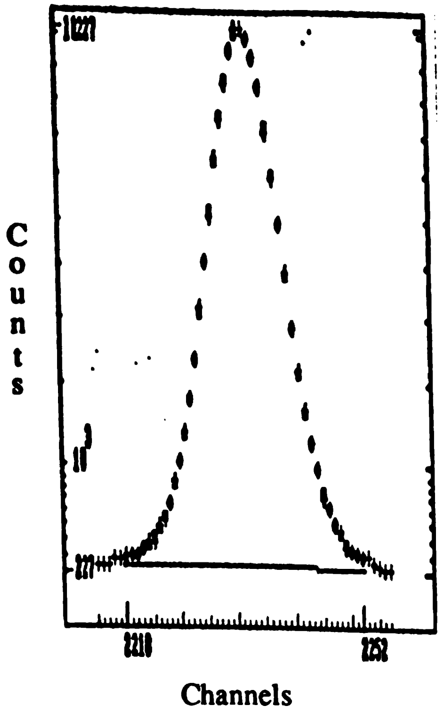

Figure 3.15 A Good Fit

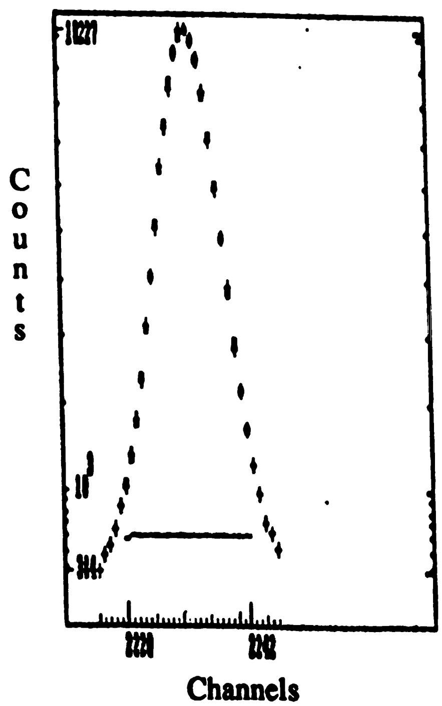

Figure 3.16 A Too Narrow Fitting Interval

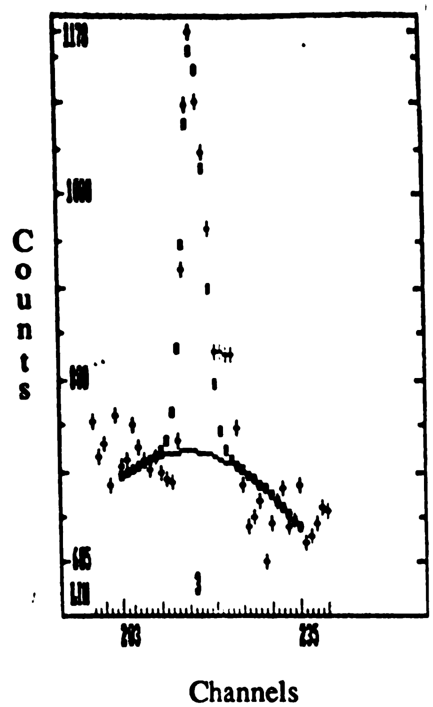

Figure 3.17A Parabolic Continuum

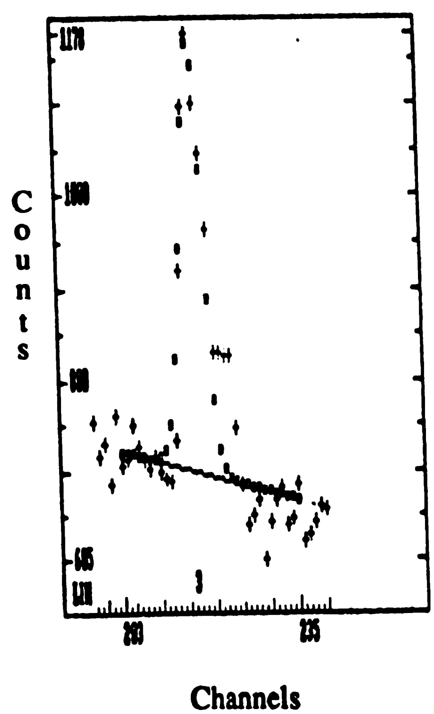

Figure 3.17B Linear Continuum

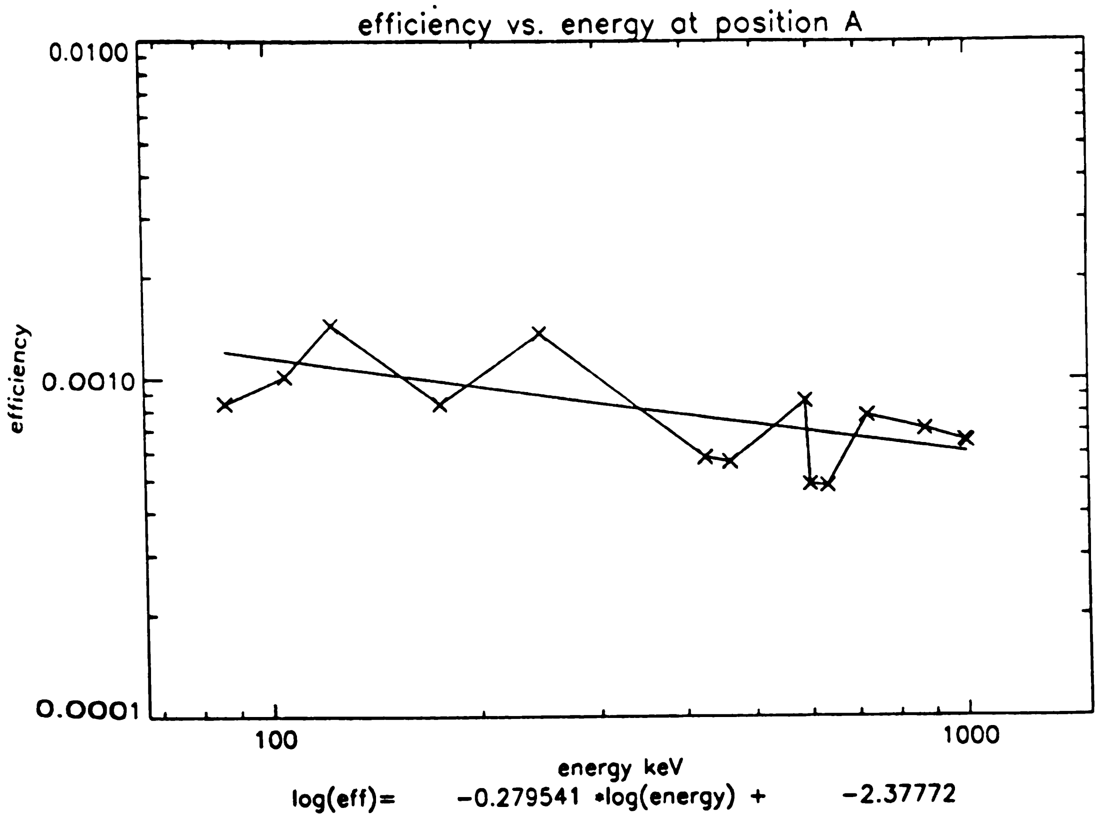

Figure 3.18 Efficiency Curve at Position A

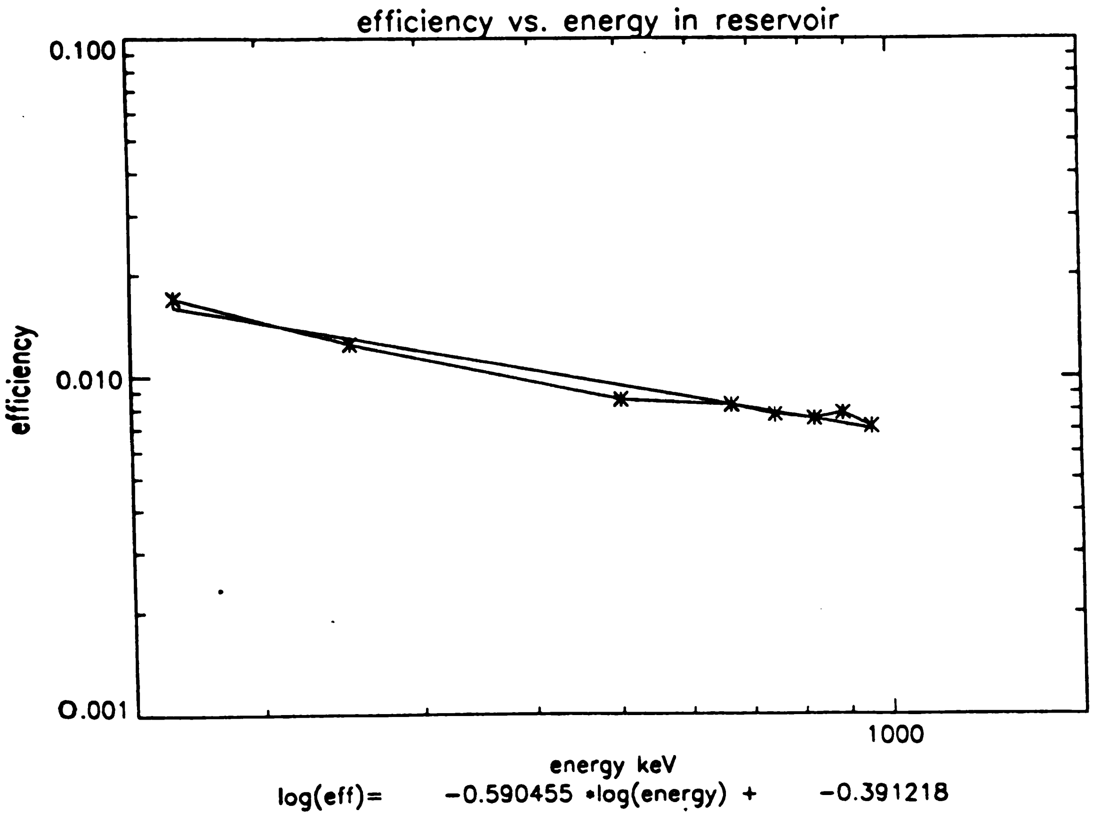

Figure 3.19 Efficiency Curve in Reservoir

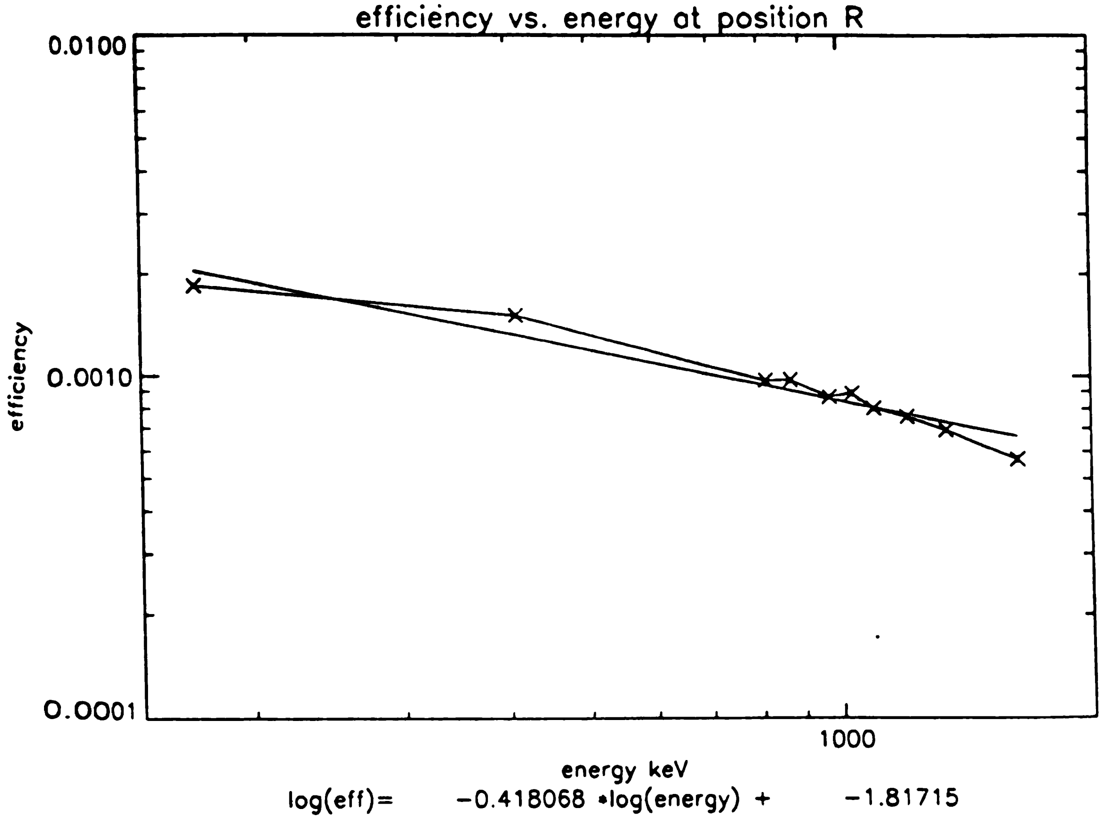

Figure 3.20 Efficiency Curve at Position R

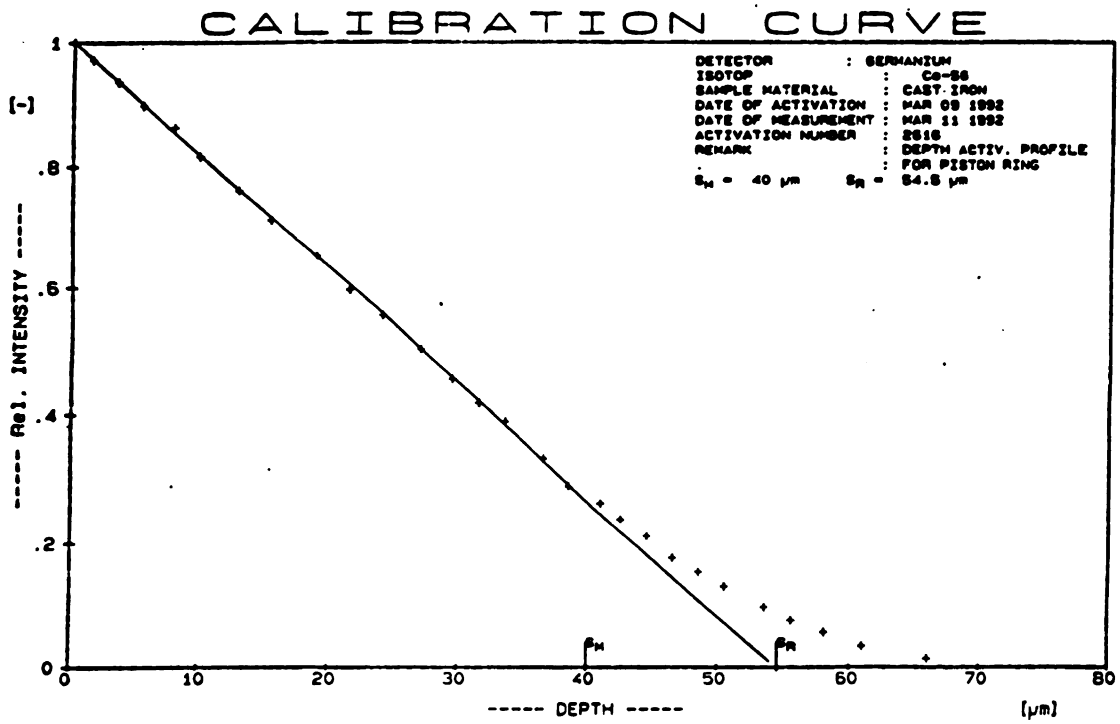

Figure 4.1 Depth Calibration Curve

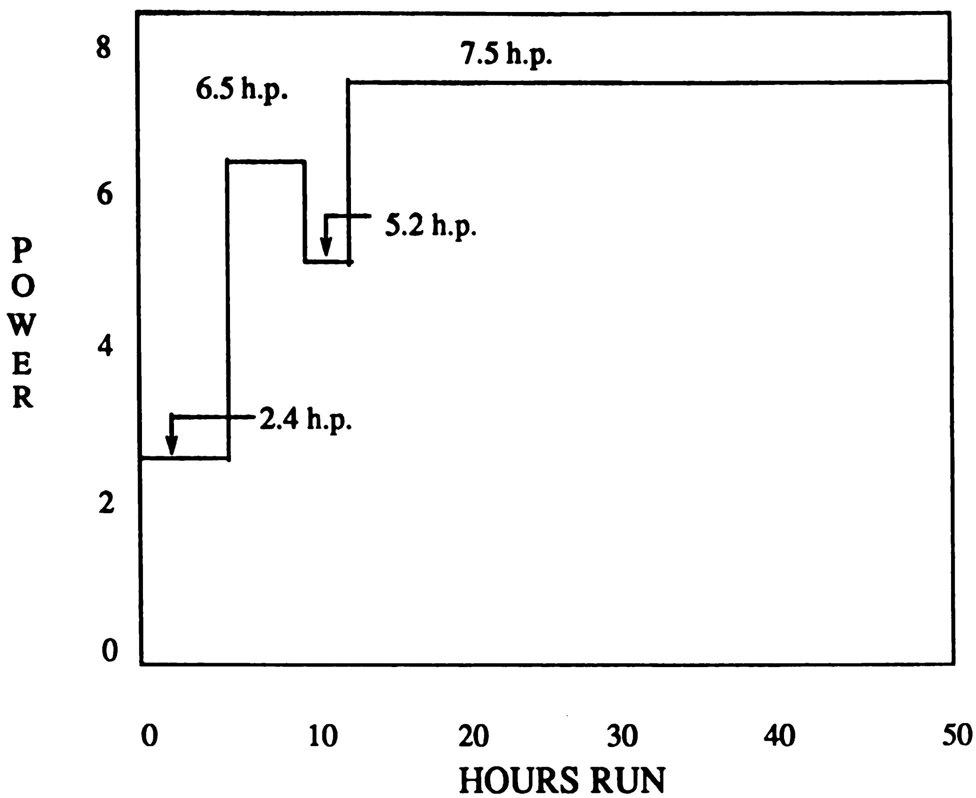

Figure 4.2 Power vs. Run TIme

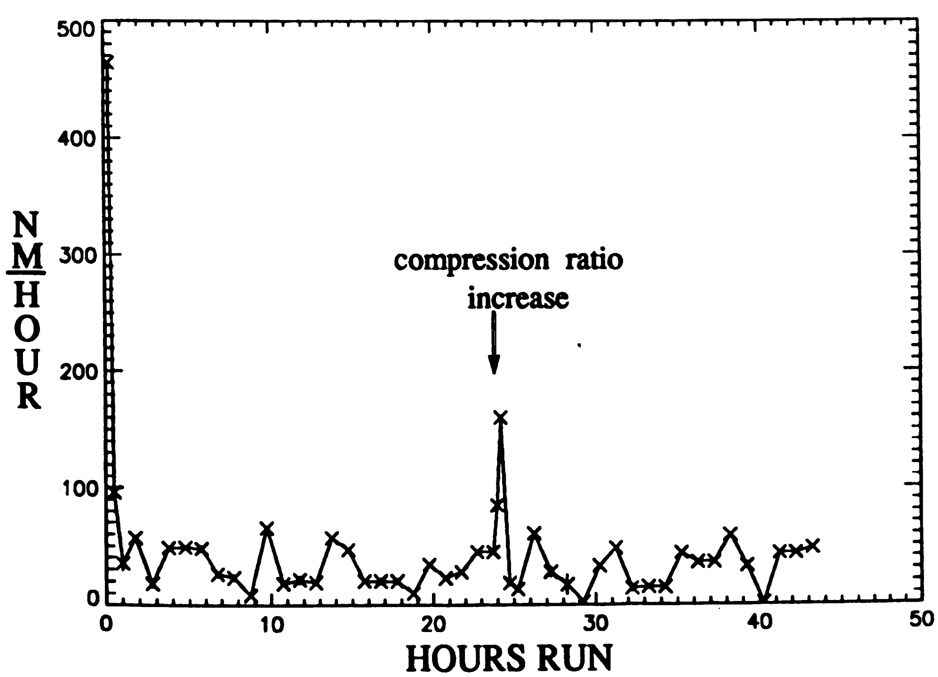

Figure 4.3 Wear Rate vs. Run Time

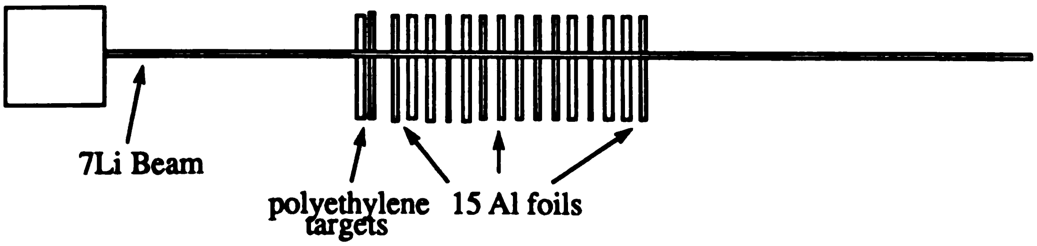

Figure B.1A 7Be Production

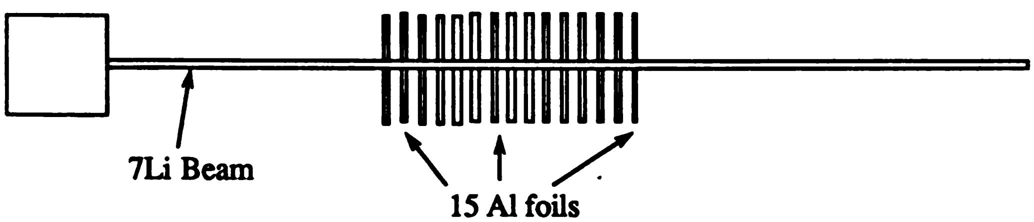

Figure B.1B 7Be Production Control

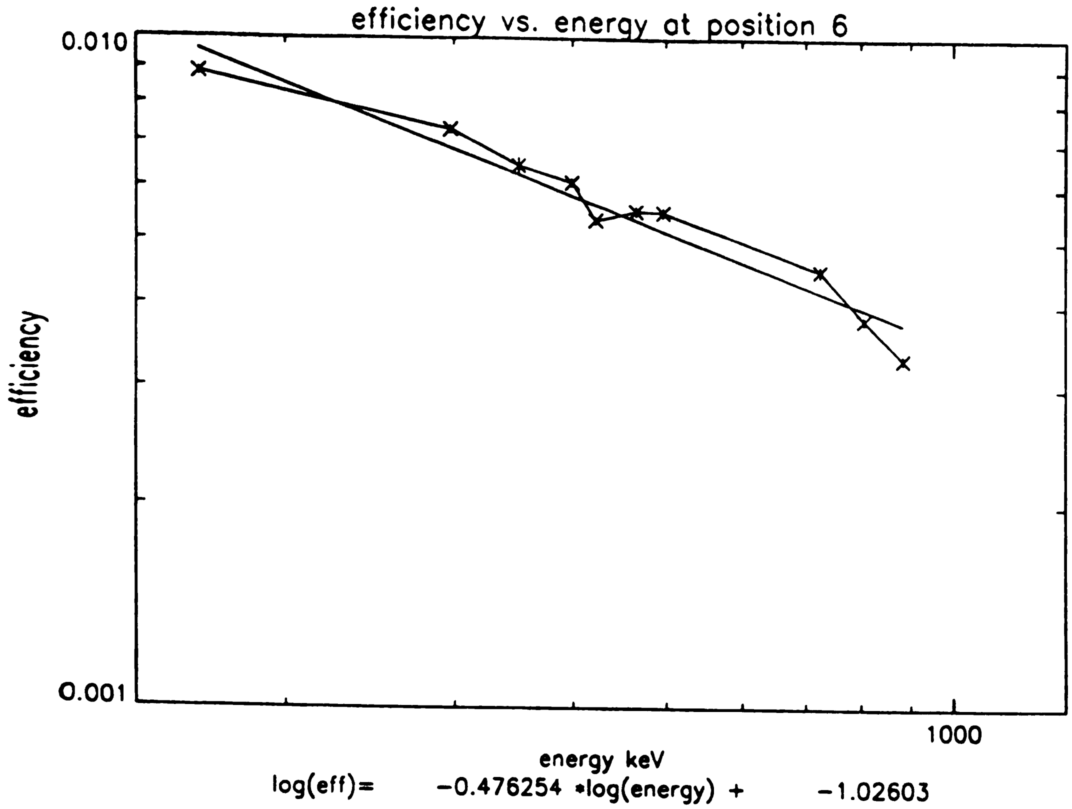

Figure B.2 Efficiency Curve at Position 6

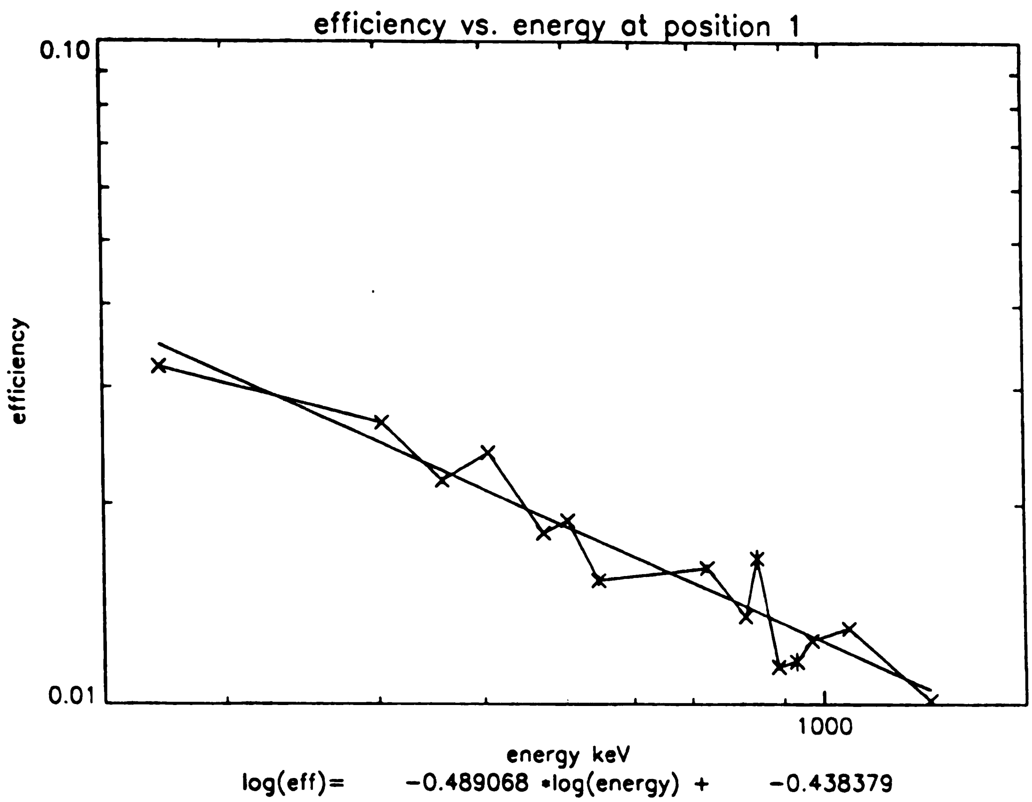

Figure B.3 Efficiency Curve at Position 1

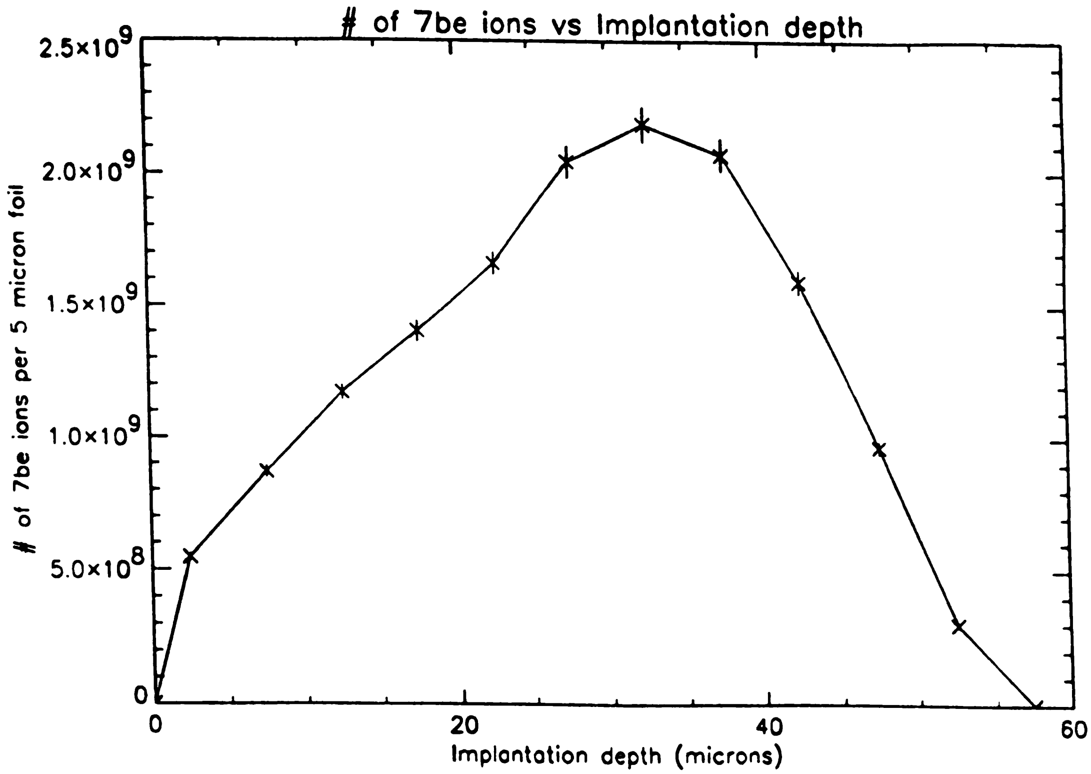

Figure B.4 Ion Distribution Curve

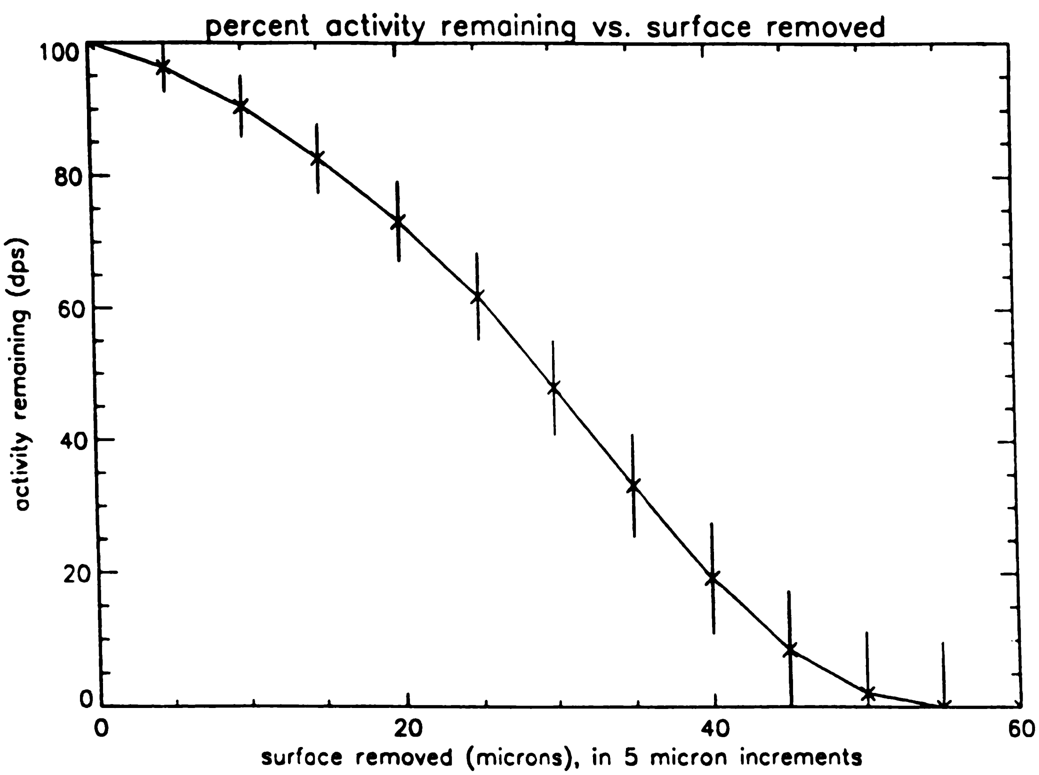

Figure B.5 Depth Calibration Curve

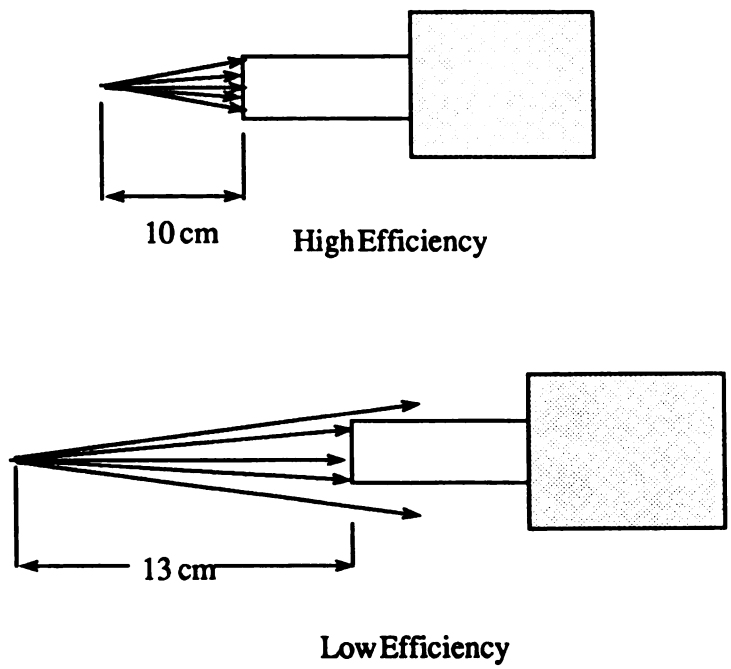

Figure C.1 Effect of Distance on Detector Efficiency

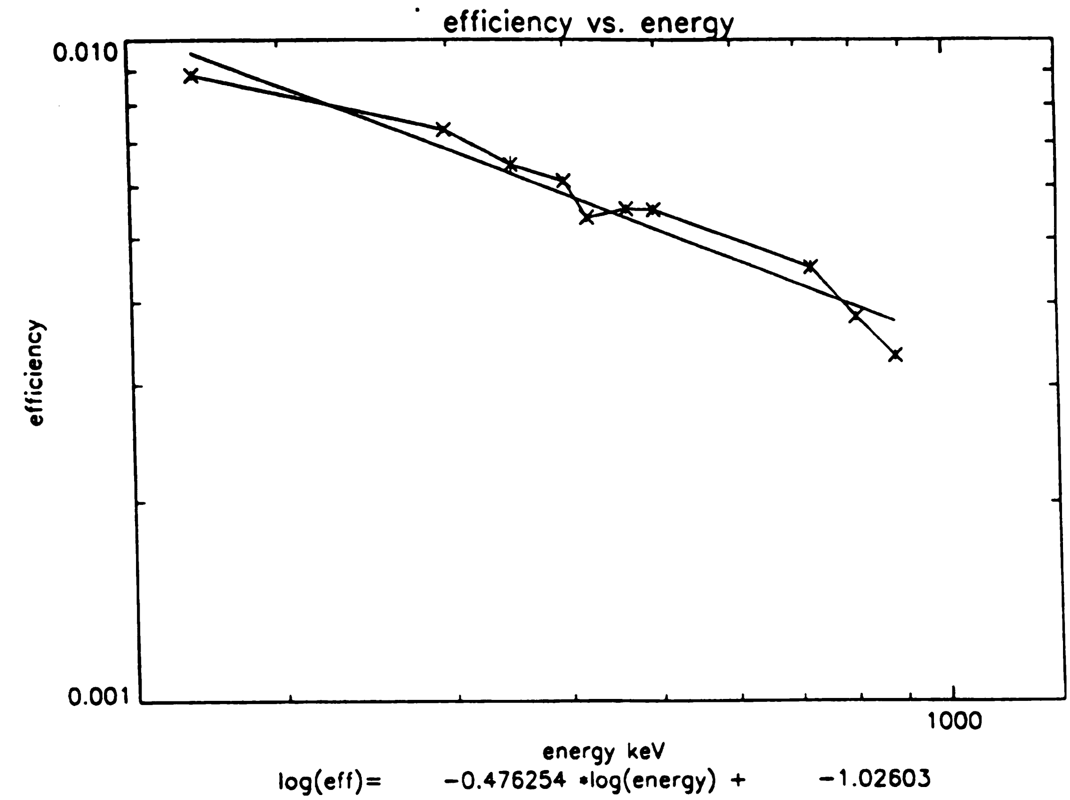

Figure C.2 Typical Efficiency Curve

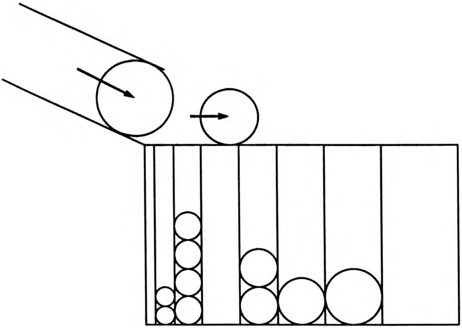

Figure C.3 Coin Bank

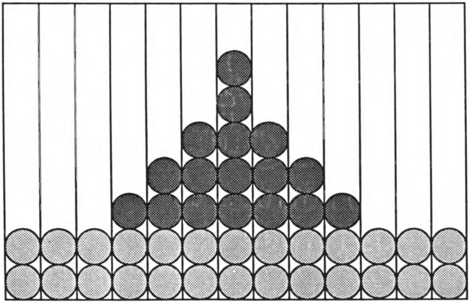

Figure C.4 Gaussian Pattern of Signal Collection

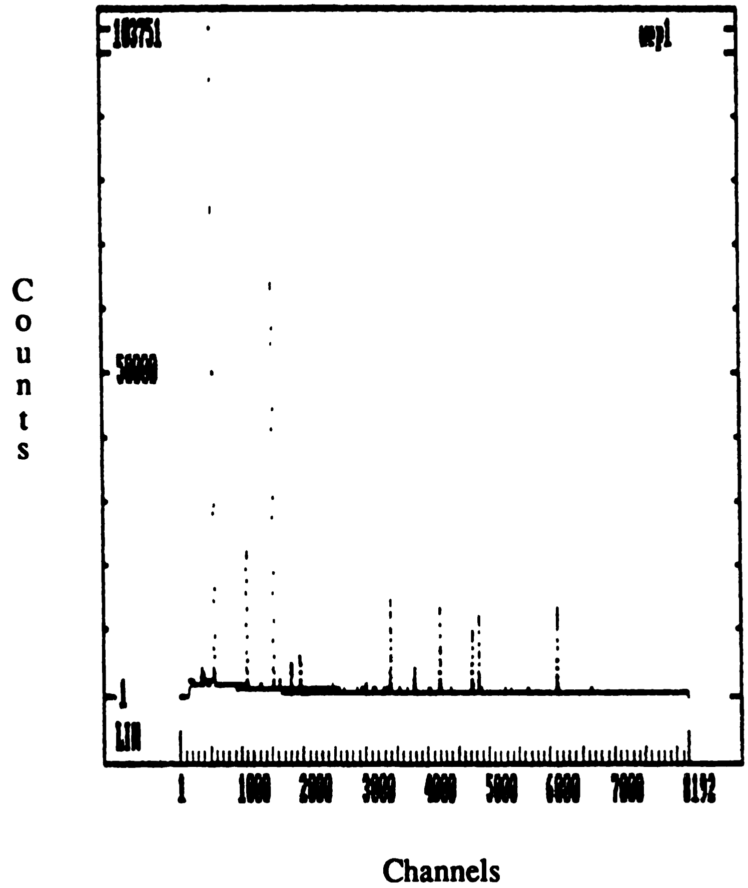

Figure C.5 Europium 152 Spectrum

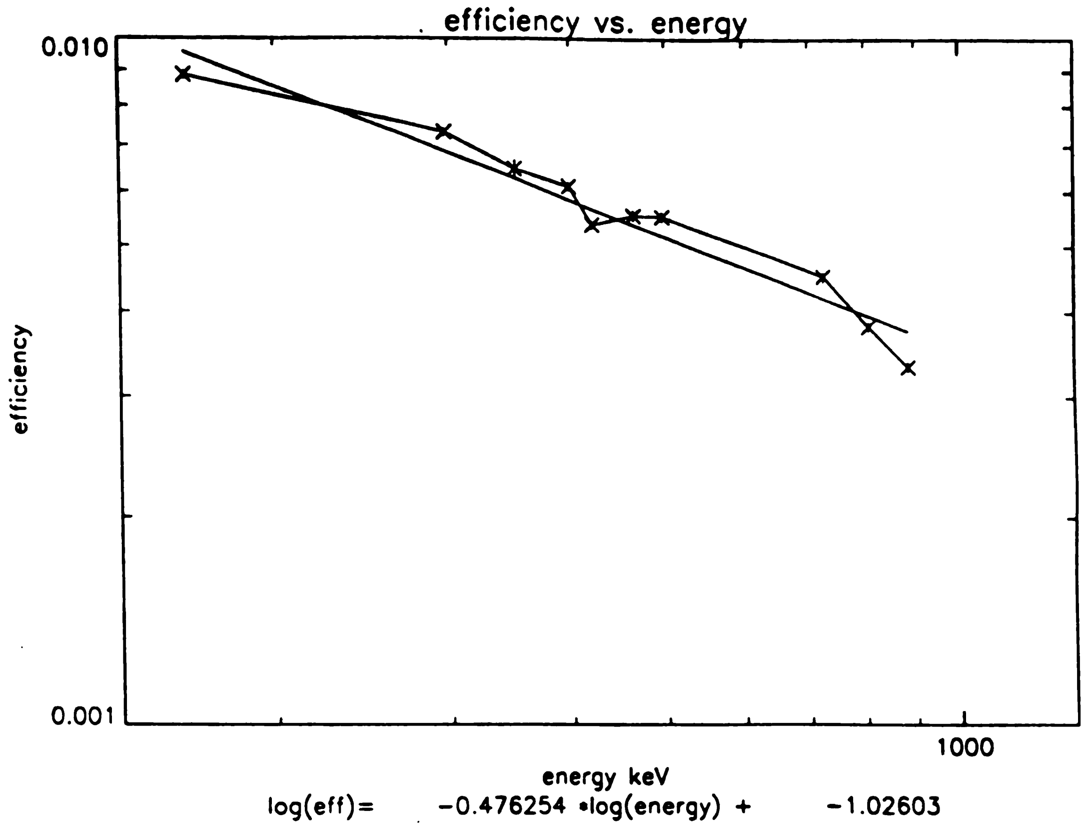

Figure C.6 Example Efficiency Curve

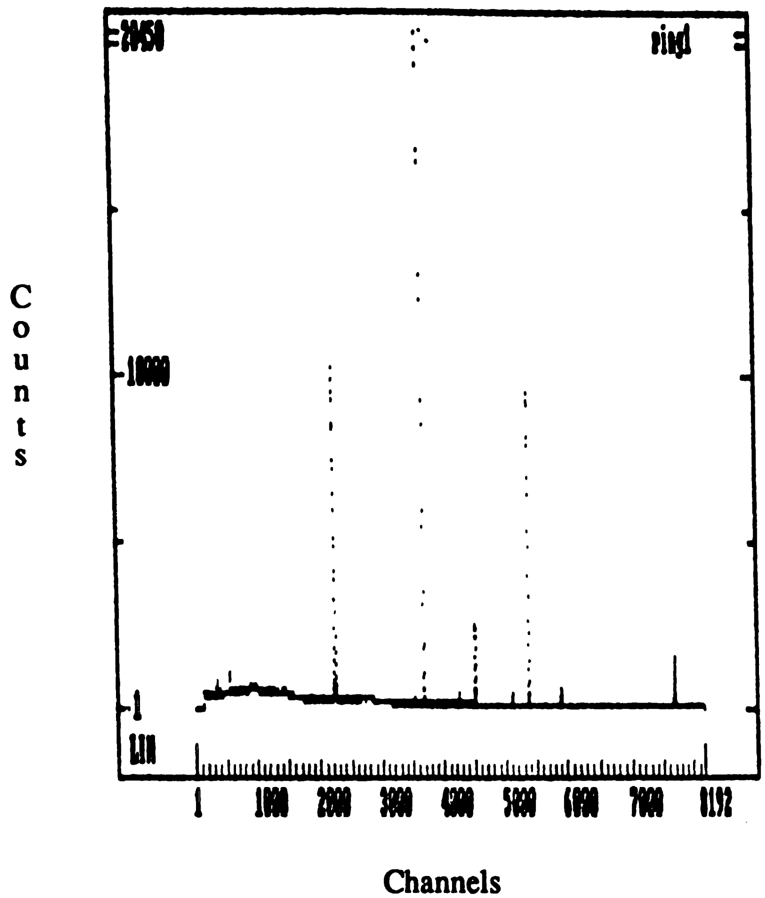

Figure C.7 Cobalt 56 Spectrum